Static and dynamic studies of foam and foam-oil interactions

Anne Kari Vikingstad

Dissertation for the degree philosophiae doctor (PhD)

University of Bergen

2006

Anne Kari Vikingstad

Centre for Integrated Petroleum Research

Department of Chemistry

University of Bergen

Allégaten 41

N-5007 Bergen

Norway

Bergen, Norway

September 2006

Preface

This thesis submitted for the degree Philosophiae Doctor at the University of Bergen, consists of five papers and two research reports along with an introduction to the work. The papers are based on work performed at the Centre for Integrated Petroleum Research at the University of Bergen in the period 2003-2006. Simulation work performed during a research period at University of Texas at Austin in spring 2005 is summarized in a research report.

The papers include different approaches to the topic of foam and foam-oil interactions. Paper 1-3 address the topic through studies of static foam experiments, whereas Paper 4 includes results from dynamic core flooding experiments. The static and dynamic foam properties of a fluorinated surfactant and alpha olefin sulfonate are compared. Paper 5 and 6 include studies of gravity segregation of foam in small scale model reservoirs, while Paper 7 is a report from a foam potential study from a field in the North Sea.

Acknowledgements

I wish to express my gratitude to my supervisors Dr.scient Morten Aarra, Professor Arne Skauge, and Professor Harald Høiland. Thank you for shearing you knowledge with me, for the many discussions during the years and for teaching me a lot of experimental procedures in the lab.

I would like to acknowledge Dr. William Rossen for including me in his research group during my stay at the University of Texas at Austin. I would also like to thank Dr. Quoc Nguyen for many good discussions. The rest of the science group in Austin is also thanked.

My fellow students and colleagues at the Centre for Integrated Petroleum Research are gratefully thanked for having a good time. Thanks for interesting discussions, and for collaboration and encouragement in the lab.

Last, but not least, I wish to thank Bjarte and the rest of my family for support and having belief in me.

List of papers

1. **Foam-oil interactions analyzed by static foam tests,**
   Anne Kari Vikingstad, Arne Skauge, Harald Høiland, and Morten G. Aarra,
   Colloids and Surfaces A: Physicochem. Eng. Aspects 260 (2005) 189.

2. **Effect of surfactant structure on foam-oil interactions**
   Comparing fluorinated surfactant and alpha olefin sulfonate in static foam tests,
   Anne Kari Vikingstad, Morten G. Aarra and Arne Skauge,
   Colloids and Surfaces A: Physicochem. Eng. Aspects 279 (2006) 105.

3. **Effect of surfactant structure on foam-oil interactions**
   Comparing low concentrations of a fluorinated surfactant and an alpha olefin sulfonate in static foam tests,
   Morten G. Aarra, Anne Kari Vikingstad, Arne Skauge and Harald Høiland,
   submitted to Colloids and Surfaces A: Physicochem. Eng. Aspects.

4. **Comparing the static and dynamic foam properties of a fluorinated and an alpha olefin sulfonate surfactant,**
   Anne Kari Vikingstad and Morten G. Aarra,
   submitted to Journal of Petroleum Science and Engineering.

5. **Gravity segregation of foam using different injection methods,**
   Anne Kari Vikingstad, research report from University of Texas, spring 2005.

6. **Injection Strategies To Overcome Gravity Segregation**
   in Simultaneous Gas and Liquid Injection Into Homogeneous Reservoirs,
   W. R. Rossen, C. J. van Duijn, Q. P. Nguyen, A. K. Vikingstad,
   presented at the SPE Improved Oil Recovery Symposium, Tulsa, April 2006.
   SPE 99794.

7. **Evaluation of Foam Potential in a North Sea reservoir**
   Production well foam treatment and Injection well foam simulations,
   Anne Kari Vikingstad, Morten G. Aarra,
   research report for Norsk Hydro, January 2006.

Contents

1 Introduction

This thesis focuses on the properties of foam, especially foam properties related to foam-oil interactions. Foam is a mix of gas, water and a foamer where the large gas volume is dispersed as bubbles in a continuous liquid phase (Figure 1). Since the foam is thermodynamic unstable, it is important to predict or investigate the foam stability.

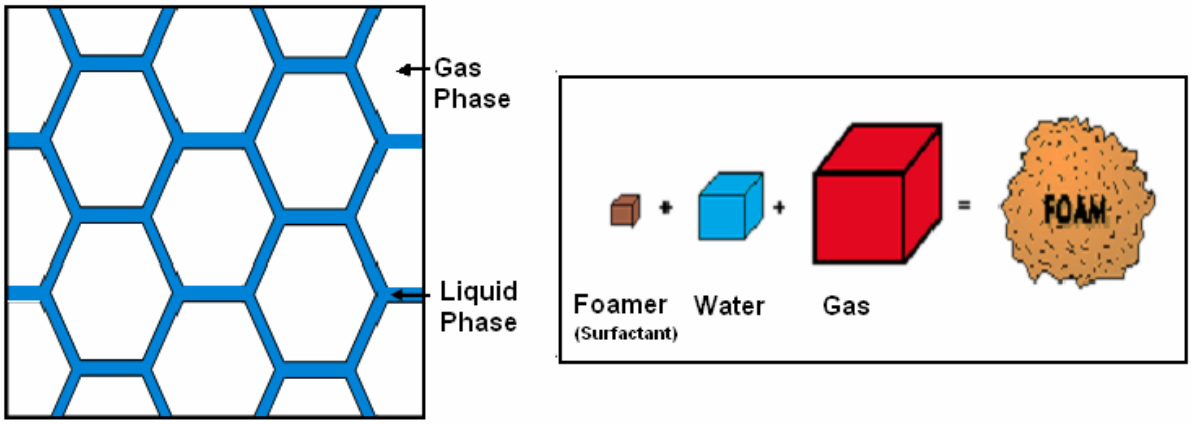

Figure 1: Illustration of foam structure and foam components.

The fundamental understanding of foam has expanded during the last decades. There have been significant advances in applications and understanding of its nature and physical behavior. Bikerman (1973) presented basic foam theory and describe a variety of experimental methods. Schramm (1994[B], 2005), Prud'homme and Kahn (1996), and Exerowa and Kruglyakov (1998) presents a wide range of fundamental foam theory and different technical applications involving foam, that will be discussed later in relation to this study.

Foam is today widely applied in a large variety of industrial branches. For instance foam can be used to improve gas sweep efficiency in a reservoir or to shut off gas production in a well. This can increase oil production. Several of the field projects have been successful, both technically and economically (Aarra et al., 1996, 2002, Aarra and Skauge, 2000, Blaker et al., 2002). Other examples are the use of foam in fire fighting, in environmental remediation processes, and in many everyday personal

care products. In enhanced oil recovery and in environmental remediation processes foam is used to control mobility. To achieve good mobility control it is important that the foam is stable. One of the key questions of foam stability is the tolerance in the presence of oil. Foam can be stable in presence of oil or oil can destabilize the foam. The properties of the oil are important for whether it will be stabilizing or destabilizing. Foam-oil interaction is a complex phenomenon, which is not yet fully understood.

In this thesis several important issues of foam have been investigated systematically, changing a few parameters at a time. This work has especially focused on trying to get a better understanding of foam-oil interactions, foam stability, and foam propagation, which are important factors for the different applications mentioned. This study adds new results to these areas and hopefully contributes to an increased understanding in different fields of foam.

This thesis first presents some fundamental theory. The theory has been included to describe foam and related foam phenomena more carefully, and to support the discussion.

In order to understand the influence of oil on foam, fundamental experimental studies were performed. This thesis has investigated foam systematically, beginning with fundamental static bulk foam tests. Main findings in these static experiments were further investigated in dynamic core flooding experiments. In addition simulations of foam gravity segregation have been preformed in a small scale model (length scale = 15-150 m x 3-30 m). The gas and liquid phases mixed in the foam will, due to buoyancy, separate in different flow paths after some distance. An extended segregation length may improve the area sweep and thereby improve the oil production. Simulations are also important for prediction of foam potential in a reservoir. The thesis also includes a foam potential evaluation simulations of a North Sea field.

The first three papers in the thesis mainly present results from static foam tests. The first paper, Paper 1, considers foam-oil interactions using an alpha olefin sulfonate. The static foam properties have been investigated by variation in surfactant concentration, amount of added oil, and variation in polarity of the oil phase. In the second paper, Paper 2, results from static foam experiments using a fluorinated surfactant are compared to the foam tests results from Paper 1. The third paper, Paper 3, presents and compares static foam experiments using a low surfactant concentration of fluorinated surfactant or alpha olefin sulfonate. The static foam properties for the two surfactants were investigated by using different low surfactant concentrations, varying amounts of different alkanes as well as crude oils. Bulk surfactant solution properties were measured to try to get a better understanding of foam stability, and to try to identify any correlations between bulk properties and foam stability.

In the forth paper, Paper 4, dynamic core flooding experiments using each of the two surfactants are discussed. The core flooding experiments in porous media (Berea cores) are performed at 120 bar and 50° C. Experiments were made with three different crude oils, all from North Sea oil reservoirs, and in addition experiments was made without oil. The sequence of experiments described was completed with the two different surfactants utilized in this thesis. Results from these dynamic flooding experiments are compared to the static bulk foam results.

Paper 5 and Paper 6 consider foam simulation experiments to investigate gravity segregation of injected liquid and gas. Especially we have focused on different injection methods influence on the gravity segregation length in cylindrical, homogenous reservoirs. The main issue for these experiments was to see if non-uniform co-injection of water and gas or injection of water above gas improved the gravity segregation of foam in a reservoir, compared to uniform co-injection. Several injection methods were considered in the foam simulations using the STARS simulator from CMG.

In the last paper, Paper 7, application of foam treatment is investigated. The simulation study includes a production well treatment and also an injection well treatment. The case study is a section of a North Sea oil reservoir.

Theory

2 Surfactant

2.1 Basic Principles

A surfactant is a molecule that has a hydrophobic hydrocarbon chain and a hydrophilic head group, see Figure 2. The surfactant can be anionic, cationic or zwitterionic. Surfactants are surface active components, and will therefore have a great influence on the surface or interfacial properties in a solution. In this study a C_{14}-C_{16} alpha olefin sulfonate (AOS) and a Perfluoroalkyl betaine (FS-500) have been used. The AOS is an anionic surfactant and FS-500 is zwitterionic. Both surfactants are commercial available. Fluor surfactants are known to generate stable foam (Dalland et al., 1992, Mannhardt et al., 2000), and AOS has been used in several successful field applications (Aarra et al., 1997, 2002, Blaker et al., 2002, Skauge et al. 2002).

Above the critical micelle concentration (cmc) the surfactant molecules aggregate in micelles. The micelles have an ordered structure that is dependent on the hydrophilic and hydrophobic properties of the surfactant. The micelle structure is also dependent on the polarity and the composition of the solution, e.g. addition of electrolytes will reduce the cmc. The spherical shaped micelles formed at cmc can reorganize to rod-like micelles, and further into multilayer laminar structures if the surfactant concentration is increased beyond the cmc (Kodama, 1973, Porte et al., 1984, Christian and Scamehorn, 1995). See Figure 2 on the next page. Transition between the spherical micelle structure and more elongated micelles can be investigated using several types of experiments, including light-scattering, speed of sound and viscosity measurements.

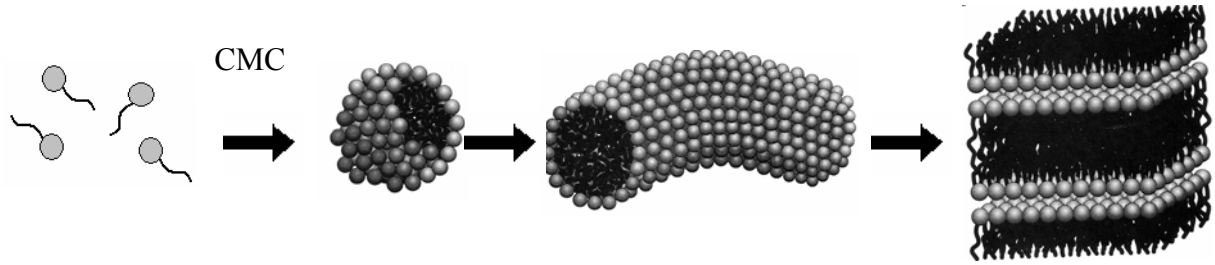

Figure 2: Different micelle structures (Evans and Wennerström, 1999)

Below cmc the movement of the water molecules is restricted due to the orientation of water molecules around the hydrophobic part of the surfactant. The ability of water molecules to move increases due to less hydrophobic interactions when the micelles are formed (Israelachvili, 1991). This transfer of the hydrophobic chain out of the water and into the interior of the micelles drives the micellization. As the surfactants head groups come close together the repulsion between them will oppose the micellization process (Evans and Wennerström, 1999). The occurrence of cmc is the result of these two competing factors.

Many physical-chemical properties, such as conductance, speed of sound and surface tension, will change dramatically when the surfactant concentration reaches the cmc. A surfactant will in general reduce the surface or interfacial tension of the solvent (Evans and Wennerström, 1999). An increasing surfactant concentration will reduce the surface tension below the critical micelle concentration, and the surface tension is approximately constant above the cmc (See Figure 1 in Paper 1). Above the cmc, an increased surfactant concentration will increase the number of micelles, while the monomer concentration remains constant.

The cmc value can be measured in many different ways (Lindman and Wennerström, 1980). In Paper 1 and Paper 2 surface tension measurements were used to find the cmc, and in Paper 3 the speed of sound method was used. Viscosity measurements and the speed of sound methods were also used to identify any transformation from spherical to more complex micelle structures in Paper 3.

2.2 Surface and interfacial tension

Surface/interfacial tension (σ) is defined as free energy (G) per area (A_G) (Atkins, 1998):

$$\sigma = \frac{dG}{dA_G} \qquad (2.1)$$

Methods that are frequently used for measuring the surface/interfacial tension are; e.g. Wilhemly plate, drop weight or volume, spinning drop and Pendant drop. A number of the most common methods are summarized and described by Schramm (2005). In this study the Pendant drop method has been used to measure the surface and interfacial tension. The Pendant drop method, and also the spinning drop method, is based on the Young-Laplace equations. The general Young-Laplace equation is given as:

$$\Delta p = p_A - p_B = \sigma_{AB}\left(\frac{1}{R_1} + \frac{1}{R_2}\right) \qquad (2.2)$$

where the pressure difference Δp is the pressure difference between pressure in phase A (p_A) and pressure in phase B (p_B). σ_{AB} is the surface/interfacial tension between phase A and phase B, and the two principal radiuses R_1 and R_2 are orthogonal and tangents of the surface.

2.3 Micellar solubilization

One of the most important properties of aqueous micellar solutions is their ability to enhance the solubility of otherwise sparingly soluble components (Høiland and Blokhus, 2003). This is referred to as the micellar solubilization process (Schramm, 1994[B]). Solubilization is relevant in many fields such as enhanced oil recovery, cosmetics, and detergents. The mechanisms for solubilization are described in detail by Christian and Scamehorn (1995), Evans and Wennerström (1999), Miller (2003),

and Høiland and Blokhus (2003). Equilibrium exists between the amount of solute solubilized in the micelles and how much simply dissolved in the water solution (Miller, 2003). The solubilization will therefore be dependent on the total solubility limit in the solution. In general large molecules are less soluble than smaller molecules.

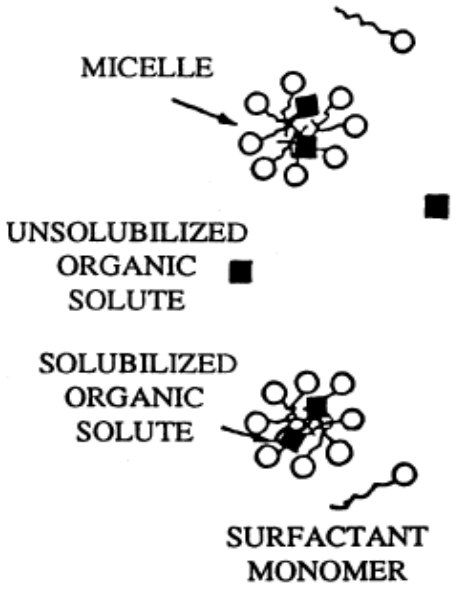

Figure 3: Solubilization of an organic component in a micelle (Christian and Scamehorn, 1995).

Nonpolar solutes such as alkanes will tend to solubilize in the micelle core, while more polar molecules will in general be anchored to the micelle surface. Addition of an alkane to a spherical micelle is expected to cause an increase in micelle volume and in the micelle aggregation number (Almgren and Swarup, 1982, Malliaris, 1987). The transition from spheres to rod like micelles usually causes moderate increase in the extent of solubility of alkanes (Christian and Scamehorn, 1995).

3 Foam

3.1 Basic Principles

Foam is a structured two phase compressible fluid with a systematic hexagonal foam texture as shown in the Figure 4 (Schramm and Wassmuth, 1994). Foam is a mix of gas, water and a foamer, and consists of liquid films/lamellas and Plateau borders. A Plateau border is the connection point of three lamellas, at an angle of 120° (Figure 4). In three dimensions, four Plateau borders meet at a point at the tetrahedral (~109°) angle. The large gas volume is dispersed as bubbles in a continuous liquid phase. The gas is in this way made discontinuous, and the gas mobility will be decreased in a porous medium. The liquid films in the foam are stabilized by surfactants to prevent bubble coalescence. Foam is thermodynamic unstable, and stability of the thin liquid films are important for foam stability.

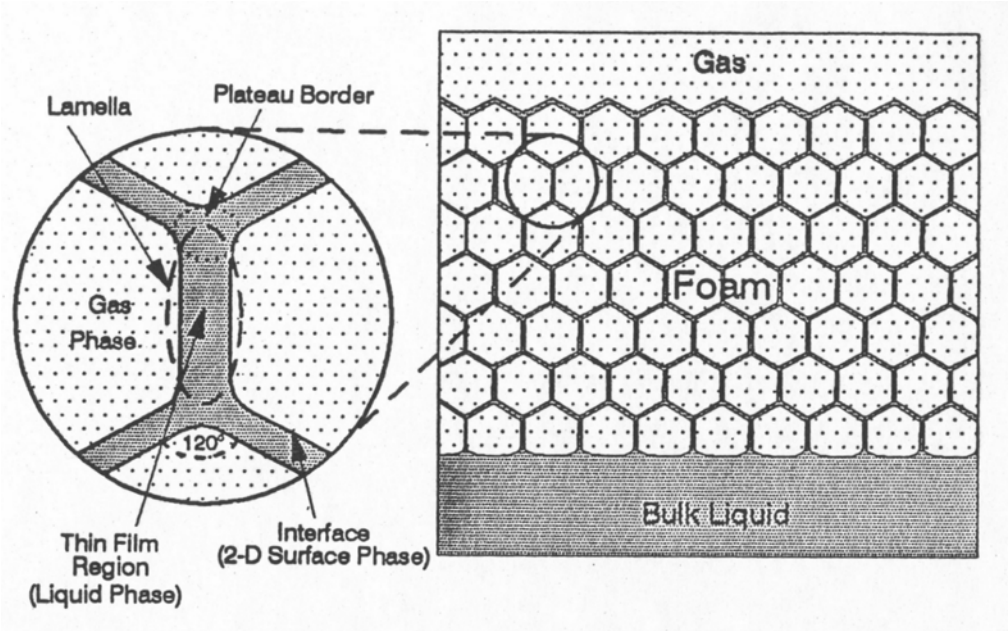

Figure 4: Illustration of a foam system in 2D (Schramm and Wassmuth, 1994)

3.2 Film stability

The stability of foam may be understood by investigating the liquid film separating two gas bubbles. Forces acting in the liquid films and the dependence on film thickness have not been measured in this thesis. However, since stability of foam is

closely connected to the stability of films and film rupture, understanding foam stability mechanisms and foam forces are a necessary foundation for understanding foam stability.

In a foam lamella the polar head groups of the surfactant are oriented into the interior of the film, and the non-polar tails toward the gas phase (Figure 5). In order to determine the stability of a foam film, thinning and coalescence have to be considered.

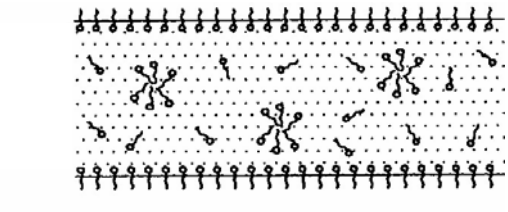

Figure 5: Foam film (Schramm and Wassmuth, 1994).

Processes and properties those are important for foam stability is gravity drainage, capillary suction, surface elasticity, surface and bulk viscosity, electric double-layer repulsion, dispersion force attraction, and steric repulsion (Schramm and Wassmuth, 1994). These processes are described in this chapter.

Foam is destabilized by capillary suction and diffusion coalescence. Immediately after foam generation the liquid will start to drain out of the lamellas (Schramm, 2005). After some time the lamellas will get more planar, and the capillary forces will become competitive to the gravity force. The pressure is lower in the Plateau borders than in the thin films. The liquid will therefore tend to flow towards the plateau borders causing thinning of the films (Figure 6). Thinning of the lamellas can lead to film rupture and coalescence of bubbles. This can cause foam collapse.

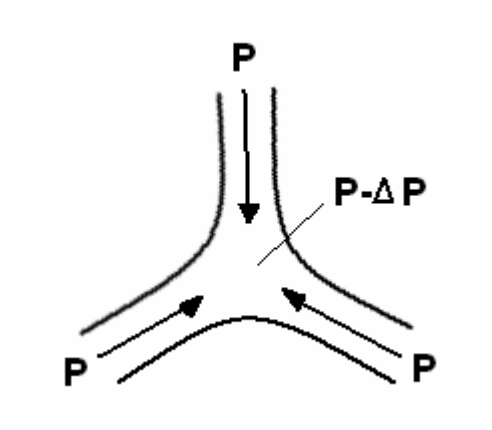

Figure 6: Pressure drop (ΔP) causes flow of liquid towards the Plateau border.

A foam film must be somewhat elastic in order to be able to withstand deformation without rupturing. If a liquid film is expanded, the surfactant concentration will decrease in the expanded area, see Figure 7. This expansion causes an increased local surface tension that provides increased resistance to further expansions, and this produces immediately contraction of the surface. Thus, the contraction induces the liquid to flow towards the film thinning area. In this way the process will tend to resist film thinning. This is called the Gibbs-Marangoni effect.

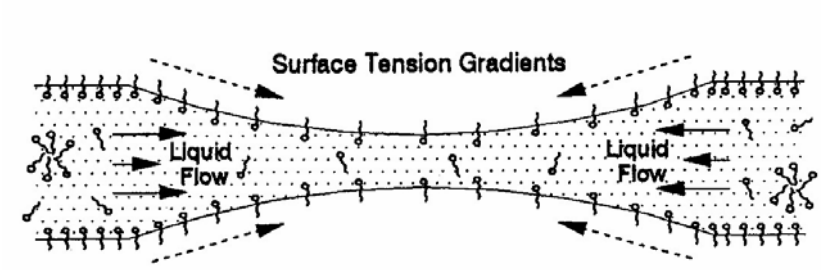

Figure 7: Surface elasticity of a foam film (Schramm and Wassmuth, 1994).

An increased surface and bulk viscosity do not normally contribute directly to stabilize the film, but rather act as resistances to the thinning and rupturing processes.

A charged interface will influence the distribution of nearby ions. Ions of opposite charge are attracted to the interface and equal charged ions are repelled. In this way an electrical double layer is formed. Because the interfaces on each side of the liquid

films are equivalent, any interfacial charge will be equally carried on each side of the film (Figure 8).

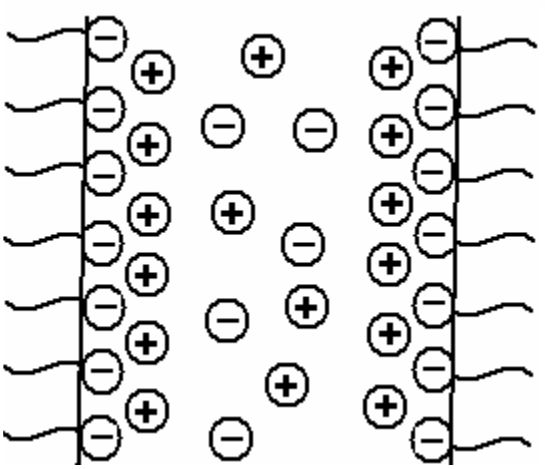

Figure 8: Eletrical double layers in a foam film.

Presence of ionic surfactants at the interface in the foam film will stabilize the film and induce a repulsive force that opposes the film thinning process. This is called the Electric double-layer repulsion (Israelachvili, 1991, Schramm and Wassmuth, 1994). The magnitude of the force will depend on the charge density and the film thickness.

The stability of a foam film separating two gas bubbles will depend on the forces that tend to disjoin or separate the two interfaces (Israelachvili, 1991). The force per unit area is called the disjoining pressure (Π). The Disjoining pressure represents the net pressure difference between the gas phase in the bubbles and the bulk phase in the lamellas. The forces that contribute to the disjoining pressure are:

1. van der Waals forces
2. electrostatic forces
3. structural/solvation forces

In the classical Derjaguin-Landau-Verwey-Overbekk (DLVO) theory, introduced around 1940, explain the interactions between two colloids using only the van der Waals and electrostatic forces. However these two forces do not include the effect of hydrogen bounding and specific ion-water interactions. The DLVO theory only

considers how electrical double layer repulsion balances against the van der Waals forces. The concepts of the early DLVO theory and complementary theory of the disjoining pressure theory are explained in further detail by Derjaguin et al. (1987) and Verwey and Overbeek (1948).

The attractive van der Waals forces, the repulsive electric double-layer forces and the structural forces are dependent on distance. The total forces will therefore vary in magnitude as well as in sign, depending on the film thickness, see Figure 9. Overlapping of charged surfaces give rise to repulsive or attractive structural forces, depending on the type of structural features and on the specific changes in the structure of the liquid in the overlap zone (Derjaguin et al., 1987)

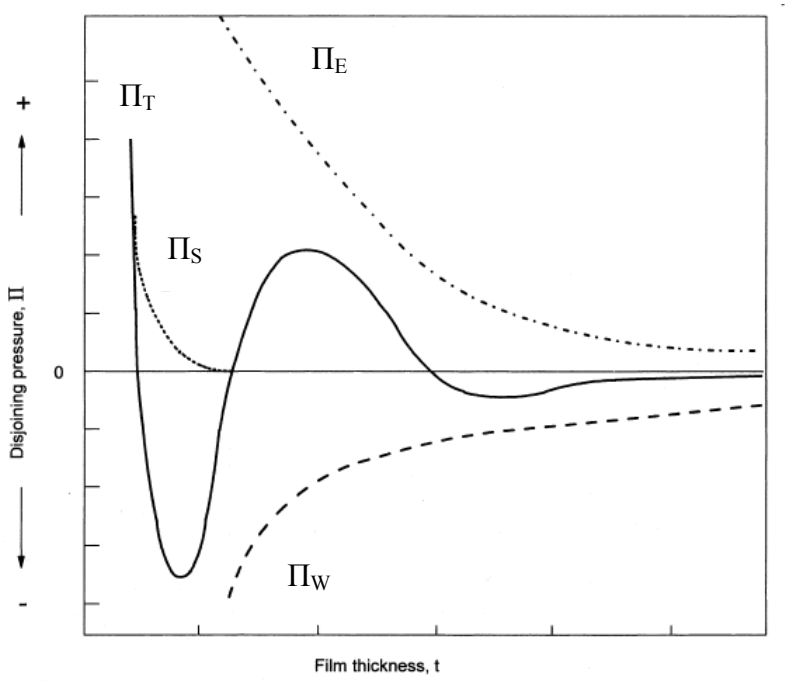

Figure 9: Illustration of disjoining pressure isotherm (Π_T) that includes contributions from electrostatic (Π_E), van der Waals forces (Π_W) and structural/steric forces (Π_S) (Schramm, 2005).

van der Waals forces: Neutral molecules exert forces of attraction on each other that are caused by electrical interactions between permanent or induced dipoles. For molecules, the force varies inversely with the sixth power of the intermolecular distance.

Electrostatic forces: Surfactant molecules are adsorbed on each of the gas-liquid interfaces in a foam film, and thereby creating charged surfaces. Gas bubbles with the liquid films between them will in this way be stabilized by the repulsive forces created when two equally charged interfaces approach each other and their electric double layers overlap.

Structural forces: In addition to the effect of hydrogen bounding and ion-water interactions, the surfactant will play an important role in the film structural forces. At surfactant concentrations several times the cmc, the structural force inside the film is important (Wasan et al., 1994). This ordered micellar structure within the film was found to enhance the film stability (Nikolov and Wasan, 1989, Nikolov et al., 1989). A long range colloid crystal like structure is formed because of the internal layering of micelles inside the film. The film will undergo a stepwise layer-by-layer film thinning process of such an ordered film structure. Below the cmc, the film formation and lifetime are dependent on the capillary pressure. In this way the thinning process of a lamella is dependent on the surfactant concentration. Mechanisms of thinning processes are described in further detail by Wasan et al. (1994). The structural forces are shorter ranged than the van der Waals and electrostatic forces.

3.3 Foam Stability in presence of oil

Presence of oil may influence the foam stability. Model oils, e.g. alkanes, are often used to investigate foam-oil interactions. Since their composition and basic properties are well known, they can be used to examine specific effects in foam-oil interactions, e.g. molecular weight variation. Crude oils have complex compositions and properties. They consist of different hydrocarbons, small amounts of oxygen, sulfur and nitrogen and also some components that contain different metals (Speight, 1998). The hydrocarbons contain different amounts of paraffin, aromatics and naphtene, and have different physical and chemical properties e.g. viscosity and density.

Oil can be solubilized in the micelles, or it can remain as emulsions or as a continuous oil phase in the liquid films. The orientation of the oil and the properties

of the oil are important for whether or not the oil will influence the foam. The dependence on surfactant concentration, brine composition, temperature and pressure are also important for the foam stability in presence of oil. There are four main theories for explaining foam stability in presence of oil:

1. Spreading and entering coefficients
2. Lamella number
3. Bridging coefficient
4. Pseudo-emulsion film theory.

3.3.1 Spreading and entering coefficients

In the literature foam stability in the presence of oil is related to a negative entering coefficient (***E***) which implies a negative spreading coefficient (***S***) (Schramm, 1994, Aarra et al., 1997, Mannhardt and Svorstøl, 1999, Mannhardt et al., 2000). The spreading and entering coefficients are calculated by using interfacial and surface tensions:

$$S = \sigma_{w/g} - \sigma_{w/o} - \sigma_{o/g} \qquad \textbf{(3.1)}$$

$$E = \sigma_{w/g} + \sigma_{w/o} - \sigma_{o/g} \qquad \textbf{(3.2)}$$

$\boldsymbol{\sigma_{w/g}}$ is the surface tension between water and gas, $\boldsymbol{\sigma_{w/o}}$ is the interfacial tension between water and oil, and $\boldsymbol{\sigma_{o/g}}$ is the surface tension between oil and gas.

By definition the oil will spread at the surface and break the foam if the spreading coefficient is positive. If the spreading coefficient is negative, the oil will remain as a droplet at the surface, and this is by theory a necessary condition for stable foam. Rowlinson and Widom (1984) claimed that theoretically the spreading coefficient

never can be positive at equilibrium. The non-spreading oil, S<0, and the spreading oil, S>0, scenario is illustrated in Figure 10.

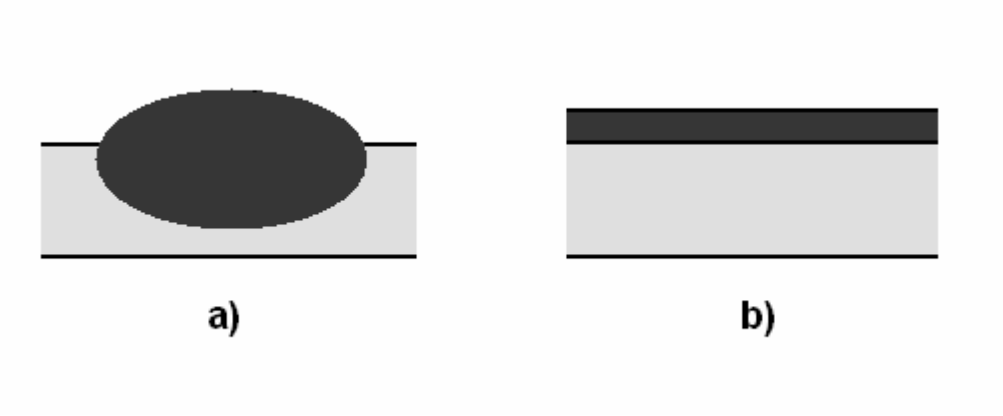

Figure 10: Illustration of: a) a non-spreading system and b) a spreading system

The role of oil spreading for antifoam activity is a subject of ongoing debate in the literature (Koczo et al., 1992, Garrett, 1993, Exerowa and Kruglyakov, 1998, Kruglyakov and Vilkova, 1999, Denkov, 2004). A good correlation is often found between antifoam ability and the positive spreading coefficient, but recent studies have raised doubts about this correlation.

3.3.2 Lamella number

The lamella number is another method of determine stability of oil transport in foam. It represents the tendency of an oil phase to become emulsified and imbibed into a foam lamella (Schramm and Novosad, 1990). A suggested simplified expression for the lamella number (***L***) is:

$$L = 0{,}15 \cdot \frac{\sigma_{w/g}}{\sigma_{w/o}} \qquad \textbf{(3.3)}$$

Based on this theory, oils can be defined to give unstable foam, moderately stable foam or they are defined to show little interaction on foam. From experiments in a microvisual cell, Schramm and Novosad (1990, 1992) have defined three types of

foams, A, B, and C. For type A foams the lamella number is less than 1, for type B foams 1<L<7, and for type C foams L> 7. Type A foams are believed to show best stability in the presence of oil, as this condition refer to both negative entering and spreading coefficients. These foams are believed to show little interactions with crude oil. Type B foams have a negative spreading coefficient and a positive entering coefficient. These foams are defined to have moderately stability to oil. Type C foams are defined to give unstable foam. Both spreading and entering coefficient are positive for these foams. Figure 11 illustrates if or how oil is imbibed in the lamella in flowing foam.

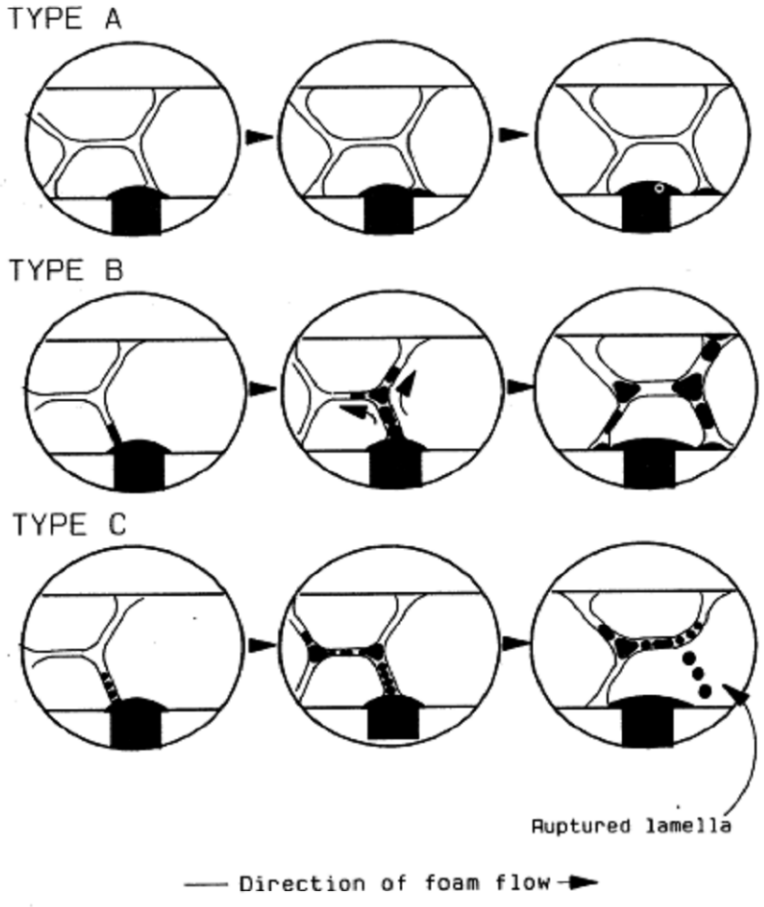

Figure 11: Illustration of type A, B and C foam, defined by the lamella number when in contact with oil (Schramm and Novosad, 1990).

3.3.3 Bridging coefficient

Another parameter often calculated when discussing antifoam efficiency of oil additives to foam is the bridging coefficient (***B***) (Garrett, 1980, Exerowa and Kruglyakov, 1998, Denkov, 2004). The equation for the bridging coefficient is given as:

$$B = \sigma_{w/g}{}^2 + \sigma_{w/o}{}^2 - \sigma_{o/g}{}^2 \qquad \textbf{(3.4)}$$

An illustration of bridging of an oil droplet in a liquid film is given in Figure 12.

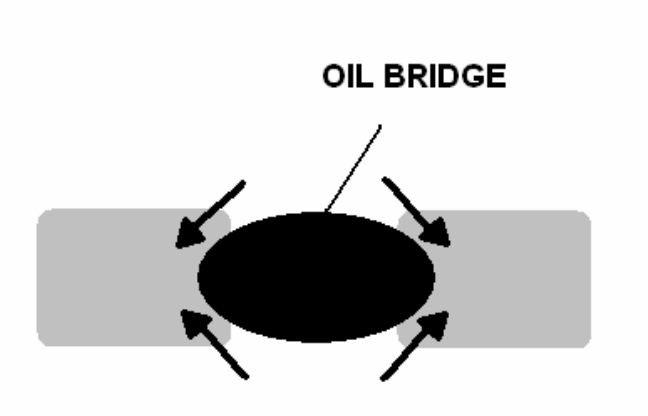

Figure 12: Illustration of an oil bridge

For the oil to behave as an antifoaming agent it is necessary, though not sufficient, that the bridging coefficient is positive. Even when the spreading coefficient is negative, the foam will become unstable once the drop has entered both the liquid films surfaces so that it spans the film, provided that the bridging coefficient is positive. A very good discussion of the bridging coefficient is given in Denkov (2004).

3.3.4 Pseudo-emulsion film theory

Raterman (1989), Manlowe and Radke (1990), Koczo et al. (1992) and Wasan et al. (1994) relate foam stability in the presence of oil to the stability of a pseudo-emulsion film. A pseudo-emulsion film is the thin liquid film between the oil droplet and the

gas phase. If the pseudo-emulsion film is stable, the oil will stay in the lamella. If the pseudo-emulsion film is ruptured, the oil may form a lens at the gas-water interface, and this can break the foam down. The creation and rupture of a pseudo-emulsion film is shown in Figure 13.

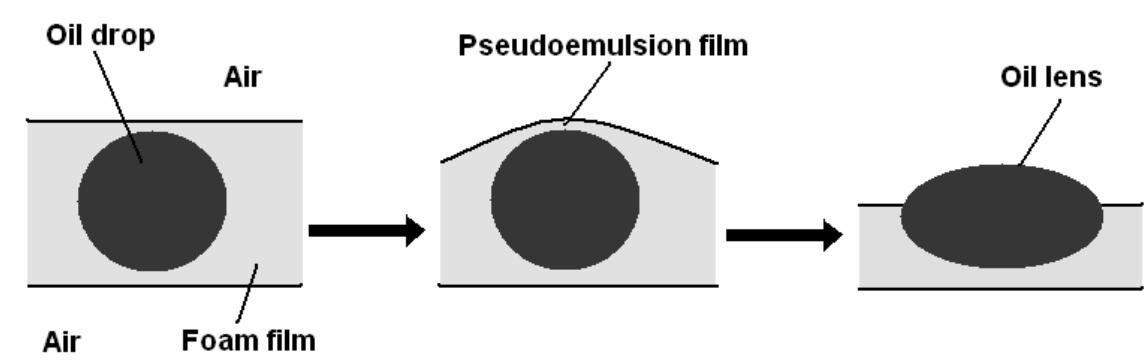

Figure 13: Pseudo-emulsion film

Lobo and Wasan (1993) reported that the pseudo-emulsion film thinned in discrete steps, which indicated the presence of an ordered micellar structure within the film. This structure was found to enhance the film stability (Lobo and Wasan, 1993).

3.4 Foam experimental methods

Bulk foam experiments, microvisual cell observations, core flooding experiments and simulations are some of the main methods used to investigate foam stability. In this study we have performed static bulk foam experiments (Paper 1-3) and dynamic core flooding experiments (Paper 4). In addition, we have simulated foam gravity segregation in model reservoirs (Paper 5-6), and estimated the foam potential in a real field case in the North Sea (Paper 7).

3.4.1 Static and dynamic bulk foam tests

The stability of bulk foam can be investigated in many different ways (Bikerman, 1973, Schramm and Wassmuth, 1994, Nishioka et al., 1996). Bulk foam experiments can be static or dynamic. The static foam height experiments presented in Paper 1-3

are performed by mixing, see Figure 14. After foam generation, the foam height decline is measured over time. Dynamic foam is one that has reached a state of dynamic equilibrium between rates of formation and decay. These experiments can be performed by continuously mixing or gas injection. Dynamic bulk foam experiments were not performed in this study.

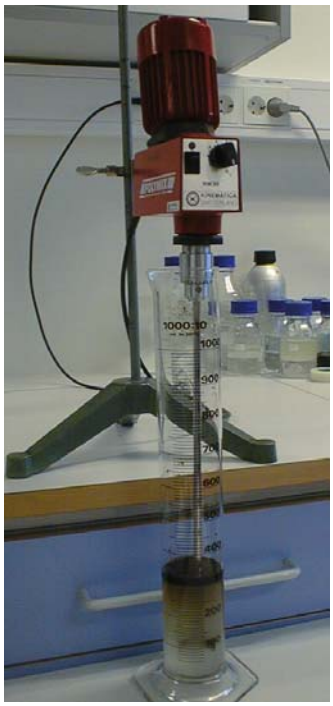

Figure 14: Experimental setup for the static bulk foam experiments

3.4.2 Microvisual cell observations

To try to increase the understanding of fluid flow in porous media, microvisual cell observations are important. A microvisual cell is a 2D simplification of a reservoir porous media. The pore network in the microvisual cell is usually enlarged compared to real core material. In microvisual cells and core flooding experiments, foam generation and foam propagation in porous media can be investigated. Fundamental bubble creation, destruction and movement are often studied in microvisual cells (Ransohoff and Radke, 1988). Foam-oil interaction is another major subject investigated in such cells (Kuhlman 1990, Schramm and Novosad, 1990, 1992, Schramm et al., 1993, Kuhlman et al., 1994). Microvisual cell experiments have not been included in this study.

3.4.3 Core flooding

Core flooding experiments with oil, at S_{orw}, and without oil were performed in this study. The results are presented in Paper 5. The experimental setup for the core flooding experiments is given in Figure 15. The pressure tabs P1-P3 are located at the inlet, outlet and about 3/5of the core length from the inlet. The experiments were conducted at 50° C and an outlet pressure of 120 bar.

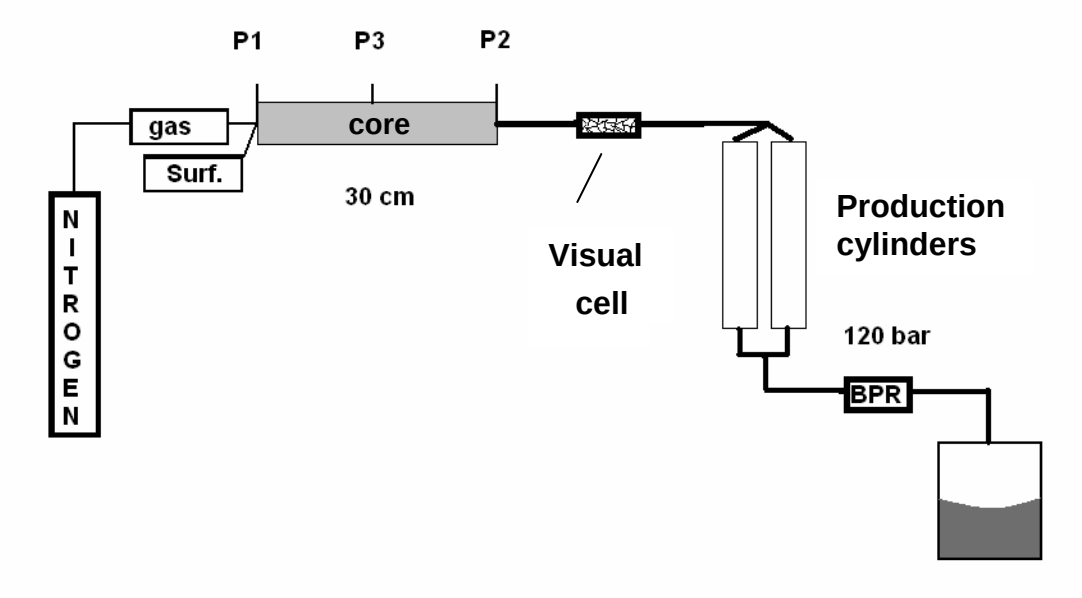

Figure 15: Experimental setup for the core flooding experiments

A great number of core flooding experiments have been performed during the years to evaluate the properties of foam stability and foam generation in the presence of oil (Schramm, 1994[B], Aarra and Skauge, 1994, Mannhardt and Svorstøl, 1999, 2001, Mannhardt et. al., 2000).

3.4.4 Simulations

Foam simulations can be used to investigate bubble movement in a capillary tube or at pore scale. Simulations can also be used in order to try to predict foam propagation in a small model or in a field reservoir. Investigation of injection methods and foam properties that may improve the sweep efficiency can also be done (Shi and Rossen, 1998, 1998[B], Rossen et al., 1999, Cheng et al., 2000). Different injection methods

influence on gravity segregation of foam was considered in Paper 5 and Paper 6. Production potential in a field is predicted by simulations (Surguchev et al., 1995, Aarra et al., 2002, Skauge et al., 2002). Foam potential simulations for a production well and an injection well treatment for a North Sea reservoir were performed in this study (Paper 7). Foam simulations will be explained in further detail in chapter 4.

3.4.5 Static and dynamic foam

Static and dynamic foam have different properties. A static foam is one in which the rate of foam formation is zero; the foam once formed, is allowed to collapse without regeneration (Nishioka et al., 1996). In such foam experiments, performed by mixing with oil present, the oil will be forced into the lamellas during mixing. After generation, the oil may drain out of the lamellas. In dynamic foam experiments foam is generated continuously. For dynamic foam in porous media the situation will be different than for static foam. If oil is present in a core and foam is injected, the foam will at some point contact the residual oil phase in the porous media. The different mechanisms described in the previous chapter will be important for the stability of the foam in presence of oil, and whether or not the oil will be present in the lamellas.

3.5 Foam in a porous media

Foam generation in porous media is dependent on injection rate and foam quality. Foam quality is the gas volume fraction of the total injected fluid rate. In a porous media the bobble size and flow are restricted by the pores. The mechanisms controlling transport and mobility of foam in porous media are complex, and a great number of different models and simulations have been done to try to better describe and understand these processes (Xu and Rossen, 2003, Chen and Yortsos, 2004). Fundamentals of foam transport in porous media are summarized by Kovseck and Radke (1994). Capillary pressure and interaction with the reservoir rock is important for foam flow in porous media (Mannhardt et al., 1998). Using some assumptions, the fractional flow theory can be applied to predict dynamic foam displacement. Fixed capillary pressure and one dimensional flow are two of the assumptions used. This is

explained in further detail by e.g. Rossen and Zhou (1995) and Rossen et al. (1999). Gauglitz et al. (2002) summarize a grate number of studies performed to examine foam generation.

Foam does not alter the water relative permeability function, but changes it indirectly by increasing the trapped gas saturation and thereby decreasing the water saturation (Bernard et al., 1965). The ability of foam to reduce gas mobility depends strongly on its texture i.e. bubble size or number of lamella per unit volume (Kovscek and Radke, 1994). Foam greatly reduces gas mobility by trapping a portion of bubbles and resisting movement of flowing bubbles. In addition, blocking of pore throats due to gas films is important (Lake, 1989).

3.5.1 Mechanisms of Lamella Creation

Foam texture is the result of competing processes of lamella creation, trapping, mobilization and destruction. The three pore-level events that lead to foam formation are snap-off, lamella division, and leave-behind, see Figure 16 - Figure 18. These processes are explained in detail by Ransohoff and Radke (1988), Kovscek and Radke (1994), and by Rossen (1996).

Lamellas are created by snap-off in the pore throats, see Figure 16. Snap-off depends on local dynamic capillary pressure in a pore throat (Rossen, 1996).

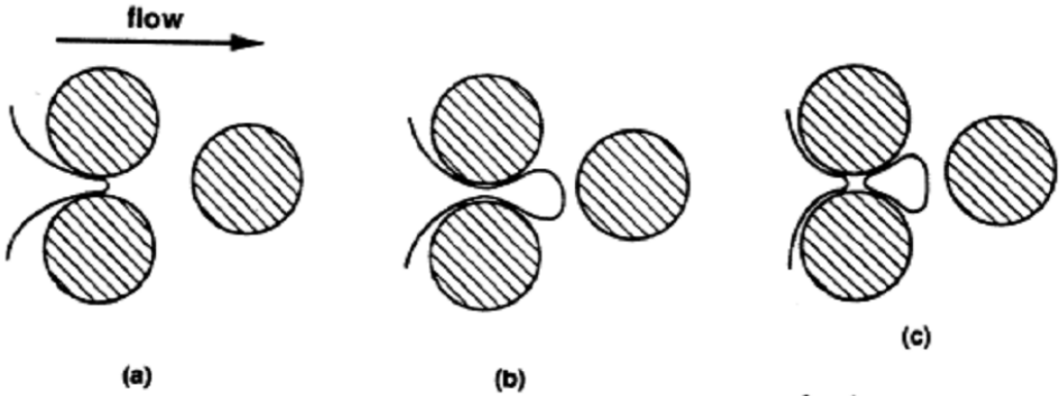

Figure 16: Schematic illustration of snap-off mechanisms: a) gas entry into liquid filled pore-throat, b) gas finger and wetting collar formation prior to breakup, c) liquid lens after snap-off (Ransohoff and Radke, 1988).

In the leave-behind process lamellas are created between neighboring pore bodies when gas enters a surfactant saturated porous medium, see Figure 17. No separate gas bubbles are formed by this foam generation mechanism, so the gas remains as a continuous phase (Ransohoff and Radke, 1988).

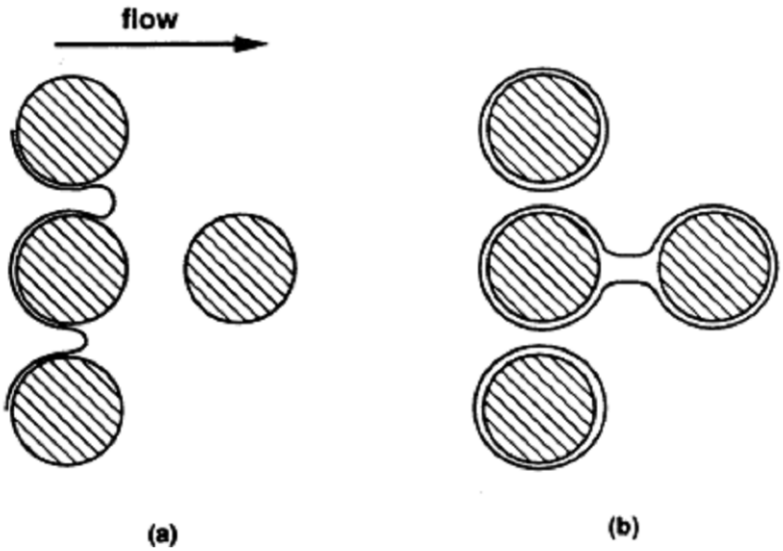

Figure 17: Schematic illustration of the leave-behind mechanism: a) gas invasion, b) stable lens (Ransohoff and Radke, 1988).

Lamella division is different from the two other generation mechanisms because it requires a moving lamella. This means that some kind of foam generation have occurred in advance. Lamella division can happen when a foam bubble splits at a

point where the flow branches in two different directions (Ransohoff and Radke, 1988), see Figure 18.

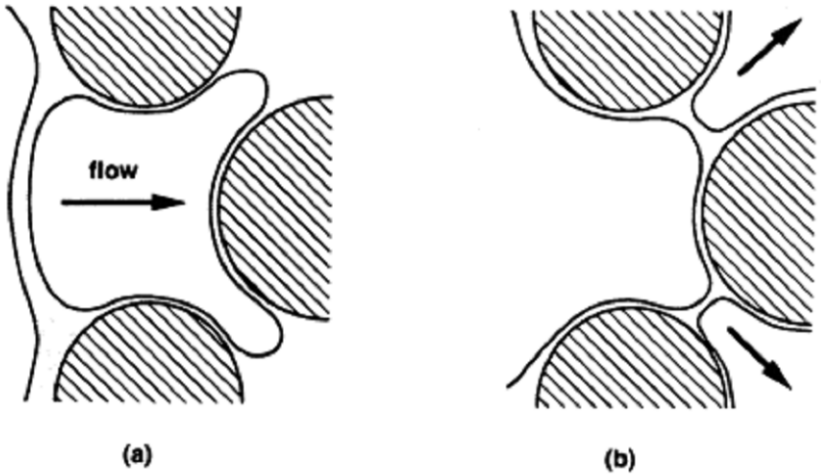

Figure 18 Schematic illustration of the lamella division mechanism: A lamella is flowing from the left to the right. a) gas bubble approaching branch point, b) divided gas bubbles (Ransohoff and Radke, 1988).

Snap-off is the dominant foam generation mechanism, especially for co-injection (Kovscek and Radke, 1994). Lamella division and leave-behind can only occur during drainage. There exists a critical velocity for homogenous porous medium above which snap-off and lamella division become the dominant generation mechanisms, causing formation of strong foam (Ransohoff and Radke, 1988). Below this velocity the foam is weaker and is caused by the leave-behind mechanism.

3.5.2 Foam Flow

There are two different models that describe gas and liquid flow in porous media: The bubble train model (Falls et. al., 1986), and the breaking-reforming model (Holm, 1968).

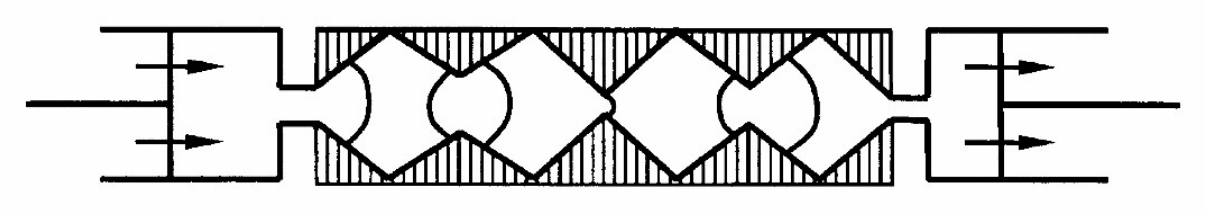

Figure 19: Schematic illustration of bubble train in porous medium (Xu and Rossen, 2003)

Falls et. al. (1986) explains the bubble train model. The gas flows in bobbles separated by the lamellas. The gas bobbles flow after each other in a long chain through the porous media.

In the breaking and reforming model the individual gas bobbles are not considered to be able to move over a large distance (Holm, 1968). The gas bobbles will therefore break and reform all the way through the porous media. The liquid flow occurs through the continuous film network of the bubbles.

3.5.3 Limiting capillary pressure and foam flow regimes

Foam flow behavior can be explained in terms of bubble texture, which is dependent on the foam film stability. The stability of a thin aqueous film depends on the average capillary pressure (p_c) defined as the difference between the gas and liquid pressures. Khatib et al. (1988) found that foam collapse occurred around a single value of p_c called the limiting capillary pressure (p_{c*}). If p_c rises above p_{c*} in a system the foam coarsens, gas mobility increases, water saturation rises, and the capillary pressure falls again. In this way a foam system regulates itself to maintain p_c near p_{c*} (Rossen, 1996). The limiting capillary pressure varies with surfactant, gas velocity, and permeability (Khatib et al., 1988). Most existing theories for foam flow regimes have used the concept of limiting capillary pressure.

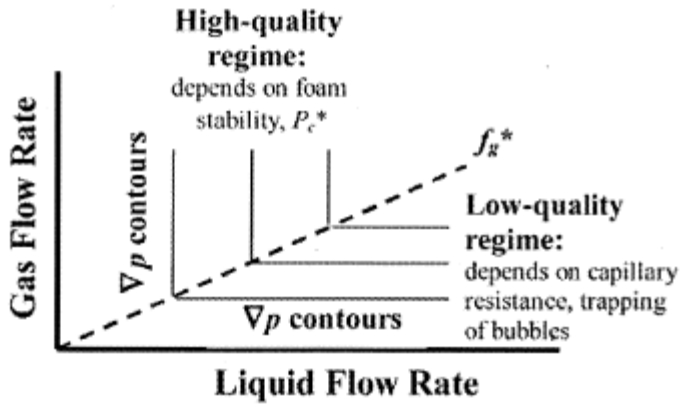

Figure 20: Schematic illustration of the effect of various factors on contour plot of the two foam regimes. The figure shows contours for several values of pressure gradients Alvarez et al. (2001).

It has been established that foam exhibits two flow regimes that are mainly governed by foam quality and total flow rate. The transition between the two regimes occurs at a specific foam quality, represented as limit gas fractional flow (f_{g*}) as shown in Figure 20. The two foam regimes were first identified by Osterloh and Jante (1992) and later confirmed to be a part of a general foam behavior (Alvarez et al., 2001). In the low-quality regime the pressure gradient is nearly independent of liquid velocity. In the high-quality regime pressure gradient is nearly independent of gas velocity. The capillary pressure is close to the limiting capillary pressure in the high-quality regime. Since p_c and water saturation (S_w) are related, S_w will remain constant in this regime as well, independent of gas and liquid flow rate (Persoff et al., 1991, Ettinger and Radke, 1992). In the model, found by Alvarez et al. (2001), the mobility was controlled by trapping and mobilization in the low-quality regime, and by coalescence in the high-quality regime. Indications of the presence of these two foam flow regimes have been found in many studies e.g. Vassenden et al. (1998[B]) and Romero et al. (2002). Polymer enhanced foams did not show this two regime behavior (Romero et al., 2002). In addition to experiments, many simulation model studies have been performed to investigate the two foam regimes (de Vries and Wit, 1990, Vassenden and Holt, 1998, Rossen et al., 1999, Cheng et al., 2000).

3.5.4 Characterizing foam

Foam can be characterized in many different ways. Visually foam can have different bubble size, bubble density and lamella thickness. In some cases it is possible to see whether or not oil is present in the liquid films. The configuration of the oil in the liquid films may also be observed. Stability of foam is another way of characterizing foam, as explained in the previous sections. In dynamic foam experiments in porous media foam is often characterized with regard to flow resistance. If two or more immiscible fluids are simultaneous flowing through the porous media, such as for foam, the relative permeability for each fluid is needed to describe the flow. Darcy's law can be used to calculate the fluid flow for each fluid (Marle, 1981, Lake, 1989).

$$Q_i = \frac{A \cdot k \cdot k_{ri}}{\mu_i} \cdot \frac{\Delta P_i}{\Delta L} \qquad \textbf{(3.5)}$$

In the equation above $\boldsymbol{Q_i}$ is the injection rate of phase *i*, $\boldsymbol{A}$ is the area, $\boldsymbol{k}$ is the permeability, $\boldsymbol{k_{ri}}$ is the relative permeability for phase *i*, $\boldsymbol{\mu_i}$ is the viscosity for phase *i*, $\boldsymbol{\Delta P_i}$ is the pressure difference across the porous media for phase *i*, and $\boldsymbol{\Delta L}$ is the length of the porous media. In foam *i* is gas or liquid. This equation assumes a horizontal, linear isothermal fluid flow without gravity.

To reduce the gas mobility is one of the main goals in enhanced oil recovery (Chapter 3.6.1). Gas is the discontinuous phase in a foam system, and the gas mobility will therefore be decreased in foam. The mobility is therefore another important factor for fluid flow in a porous media. The phase mobility ($\boldsymbol{\lambda_i}$) is given as:

$$\lambda_i = \frac{k \cdot k_{ri}}{\mu_i} \qquad \textbf{(3.6)}$$

To have an effective displacement process, where fluid 1 displacing fluid 2, it is beneficial to have a mobility ratio ($\boldsymbol{M}$) equal or less than 1.

$$M = \frac{\lambda_1}{\lambda_2} \qquad \textbf{(3.7)}$$

λ_1 and λ_2 are the mobility for fluid 1 and fluid 2 respectively.

To characterize the strength of the generated foam, the mobility reduction factor (***MRF***) is often defined (Schramm, 1994[B], Aarra et al., 1997, Mannhardt et. al. 2000):

$$MRF = \frac{\Delta P_{foam}}{\Delta P_{no-foam}} \qquad \textbf{(3.8)}$$

ΔP_{foam} and $\Delta P_{no\text{-}foam}$ are the measured differential pressure across the porous medium with and without foam respectively.

In the STARS simulator the MFR is named fmmob. This will be described in further detail in Chapter 4.

3.5.5 Foam-oil interactions in porous media

Foam-oil interactions in porous media are even more complex than foam-oil interactions in static foam tests. The foam forming surfactants may be adsorbed by the porous media or absorbed by the oil. Pore structure and wettability altering may also influence the foam stability. The oil may also destabilize the foam by spreading spontaneously on the foam film or by emulsifying and allowing oil drops to rupture the stabilizing interface. An illustration of spreading, entering and emulsifying in flowing foam lamellas are given in Figure 21.

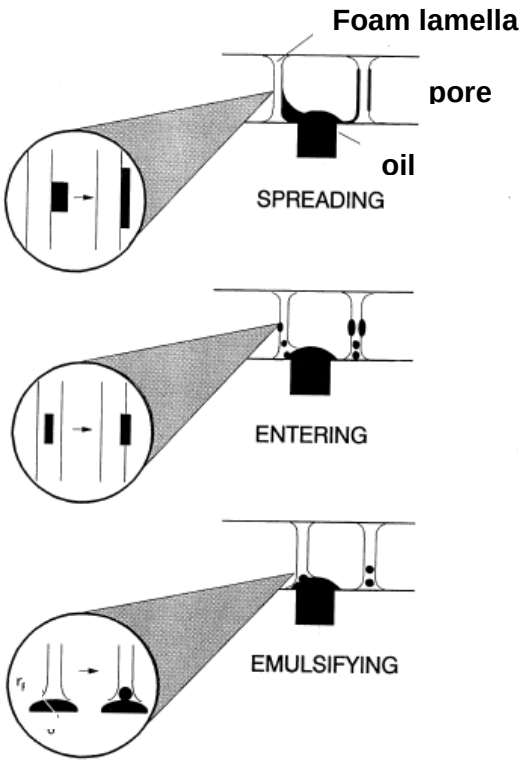

Figure 21: Illustration of interaction behaviors that can occur when foam lamella move along a thin pore and come into contact with an oil phase (Schramm and Novosad, 1990).

In the literature most data suggest that oil may limit the foam efficiency. Some define a critical oil saturation for which foam cannot be formed above (see discussion by Schramm, 1994). But several papers show that it is possible to generate strong foams at relatively high oil saturations (Aarra et. al., 1997, Mannhardt and Svorstøl 1999, Mannhardt et. al. 2000).

3.6 Foam applications

Foam has a large variety of applications. How to determine and predict foam stability are major issues for use of foam. In some applications temperature dependent stability is important, in other applications foam stability in presence of oil or other additives are important. Other important properties are foam generation rate, structure, and drainage properties. Foam can be used as mobility controller in enhanced oil recovery or environmental remediation processes, in firefighting of burning fuel, and in many everyday food and personal care products. In addition, foam can be used in mineral flotation and separation, and in textile industry.

Schramm (1994[B], 2005) and Prud'homme and Kahn (1996) presents more detailed information about these applications in their books. In this study three applications that are directly related to foam-oil interactions or mobility control are presented in further detail.

3.6.1 Enhanced oil recovery

In producing the oil from a reservoir, on average about two thirds of oil originally in place is left in the reservoir at the end of water flooding (Schramm, 2005). The use of foam to improve oil recovery includes control of gas mobility and to shut off unwanted gas production in production wells. Usually, the foam is intended to reduce gas mobility in those zones already flooded by gas.

In production wells foam can be used to shut off gas production, see Figure 22. As oil is being produced from a field, the gas oil contact will start to sink, and the gas can cone so that the well starts to produce gas instead of oil. One approach to reduce an inflow is to place a foam region around the production well. This method was used in the foam pilot test at the Oseberg Field in the North Sea (Aarra et al., 1996).

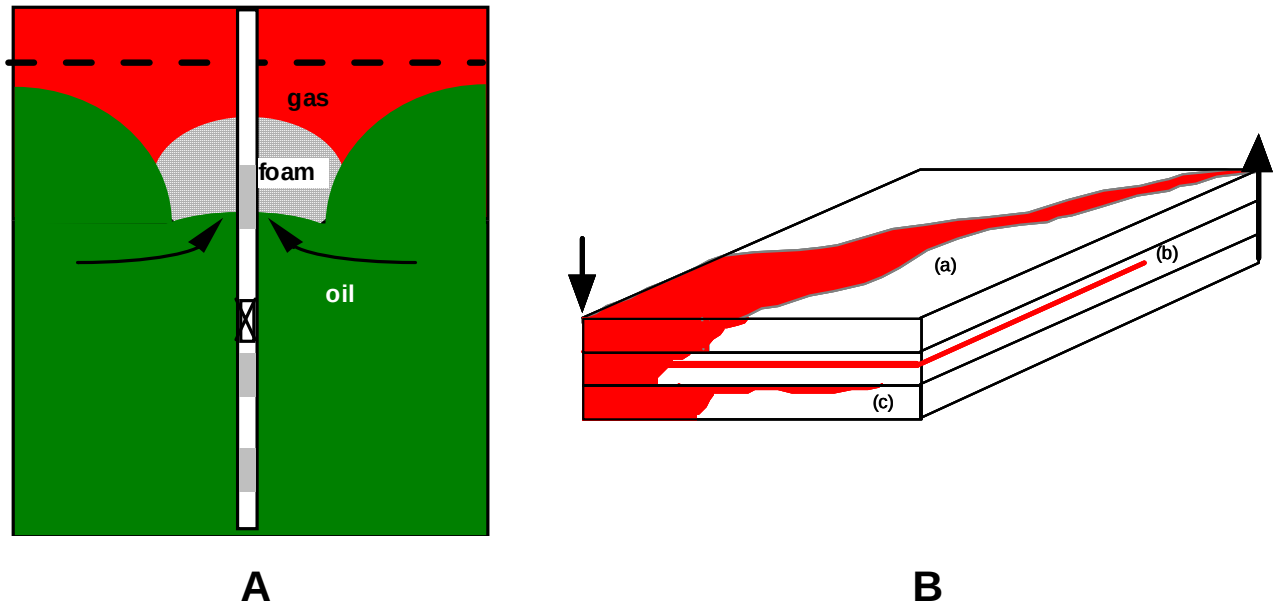

Figure 22: Illustration of how foam can be used to shut off gas production (A), and scenarios for use of foam to control gas mobility (B): a) poor area sweep, b) gas channeling and c) gravity override

Foam can also be used to improve gas sweep efficiency in a reservoir, like in the Snorre field in the North Sea (Skauge et al., 2002). Gas has low density and tends to rise to the top of the reservoir and override the oil rich zones. High gas mobility leads to viscous instability in the reservoir. By reducing the gas mobility, foam can improve problems like poor area sweep, gas channeling, and gravity override, see illustration in Figure 22. A Foam-Assisted-Water-Alternating-Gas (FAWAG) injection method is often used in injection well foam applications (Aarra et al., 2002, Blaker et al., 2002, Skauge et al. 2002).

There have been many foam field applications in the North Sea area in the recent years (Hanssen et al., 1994, Aarra et al., 1997, Chukwueke et al., 1998, Aarra and Skauge, 2000, Blaker et al., 2002, Skauge et al. 2002). Several of these projects were successful, both technically and economically. There remain, however, many challenges in the description of foam properties and in, particularly, the prediction of foam behavior. One of the most important factors in enhanced oil recovery application using foam is the influence of oil on foam stability. Foam placement is another of the critical factors for field tests. In order to understand the influence of oil saturation on foam, more fundamental experimental studies have been performed. To prepare for a field testes on the Snorre field, core flooding experiments both with (Svorstøl et al., 1996 and Mannhardt and Svorstøl, 1999) and without (Mannhardt and Svorstøl, 2001) crude oil was performed. Also large scale core flooding experiments were done to investigate foam propagation rate (Vassenden et al., 1998[B]). Several foam field applications are summarized by Hanssen et al. (1994) and Blaker et al. (2002).

3.6.2 Environment

Foam can be used in environmental remediation processes. In a surfactant/foam process for remediation of aquifers, polluted by a dense non-aqueous phase liquid pollutant, foam can be used for mobility controlled displacement of the substances that pollute the aquifer (Figure 23). Lab and field demonstration of such processes are described by Hirasaki et al. (1997, 1997[B]). It is expected that by use of only

surfactant flooding, in a heterogenic polluted field, a large portion of the solution will flow through the high permeable areas and channels, so that some pollutant is left in low permeability zones. For aquifer remediation it is not sufficient to clean the pollutant from the high permeable layers because the remaining amount will dissolve from the lower permeable layers and slowly diffuse into the ground water. In a similar way as in enhanced oil recovery, foam can be used to reduce the mobility of the injected fluid in high permeability layers. Foam may force the fluid into lower permeability layers, and thereby improve the sweep efficiency. To perform a successful remediation process, it is therefore important to know if the pollutant has any negative effect on foam stability.

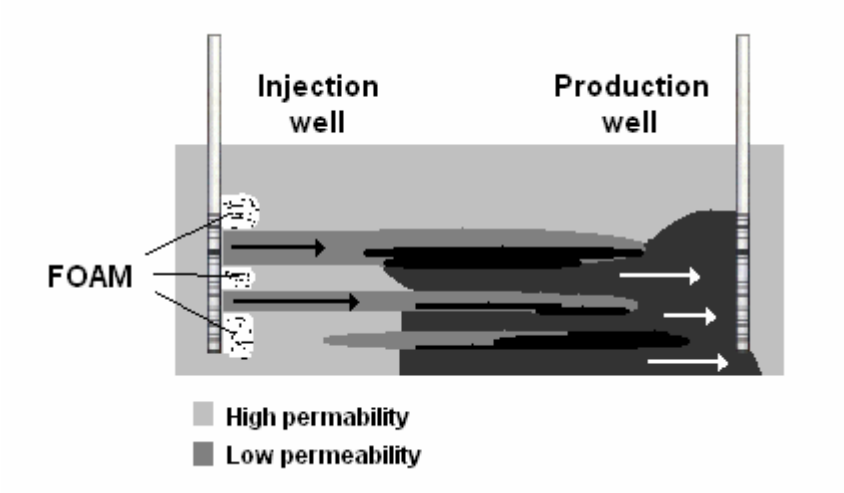

Figure 23: Illustration of foam assisted surfactant flood for the displacement and production of pollutant.

3.6.3 Fire fighting

Use of foam for firefighting is described by Briggs (1996) and Schramm (2005). Cooling the fuel below the self-igniting temperature, providing a barrier between the fuel and air, or other methods to reduce air supply, are some of the important methods to extinguish a fire (Figure 24).

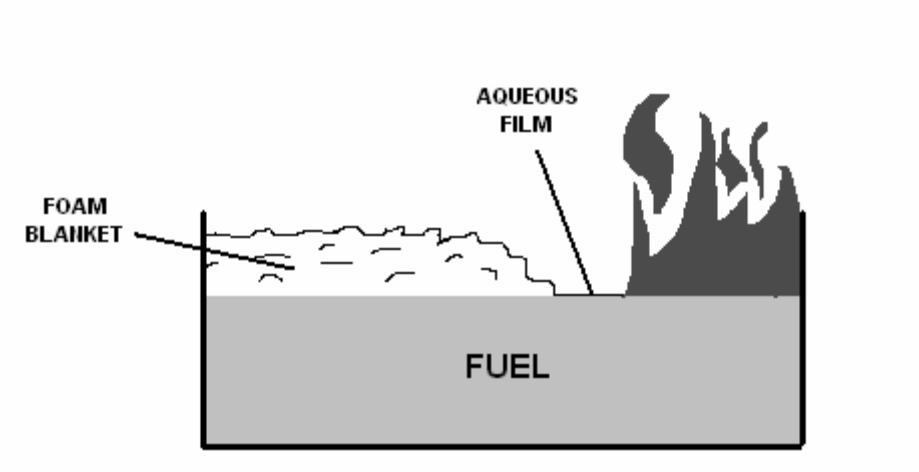

Figure 24: Illustration of the mechanisms of fire fighting foam. The foam blanket and the aqueous film will reduce oxygen supply.

Since water is denser than liquid hydrocarbons, it is likely to sink below the surface of the burning hydrocarbons and would be useless for such kind of fires. Foam has properties that make it a good firefighting agent. It has a low density and will therefore float on top of the fuel and create a barrier and thereby reduce the air supply, but foam stability in presence of the fuel is of course important. A category of fluorinated surfactants used for firefighting have interfacial characteristics, such that a thin aqueous film spread across the fuel surface. This liquid film will limit the oxygen supply. This phenomenon is hydrocarbon and temperature dependent (Briggs, 1996). Firefighting foams may also be used in non-fire situations e.g. to cover toxic spills.

4 Simulation

4.1 STARS foam model

STARS, developed by the Computer Modeling Group (CMG) of Calgary, Canada, are the most widely used commercial foam simulator. STARS is a three-phase multi component thermal and steam additive simulator. STARS can be used to simulate polymer, gel, emulsion and foam applications. For such cases the stabilized droplets or bubbles can be treated as components in the carrying phase. More complex problems like adsorption, blockage, dispersion and so forth can be considered. For simplicity, foam mobility reduction is determined through a modified gas relative permeability curve. A dimensionless interpolation factor (***FM***) is used as a weighting factor to determine gas relative permeability for a certain foam strength. The linear interpolation, FM is unity without foam, and decreases with the increasing foam strength (fmmob increases). At the lower limit of FM (i.e., FM = 0), the lowest foam mobility is determined by a reference gas relative permeability. In this sense, FM can be expressed as

$$FM = \frac{1}{1 + fmmob \cdot F_X} \qquad \textbf{(4.1)}$$

fmmob is the reference mobility reduction factor, and $\boldsymbol{F_X}$ consists of 6 dependent functions (F_1-F_6) that scale fmmob (Equation 4.2 and 4.3).

$$F_X = F_1 + F_2 + F_3 + F_4 + F_5 + F_6 \qquad \textbf{(4.2)}$$

The Functions $\boldsymbol{F_1}$-$\boldsymbol{F_6}$ are dependent on the following properties; surfactant concentration, water saturation, oil saturation, gas velocity, capillary number and critical capillary number, respectively.

$$F_X = \left(\frac{W_s}{fmsurf} \right)^{epsurf} + \left(0{,}5 + \frac{\arctan\left(epdry \cdot \left(S_W - fmdry\right)\right)}{\pi} \right) + \left(\frac{fmoil - S_O}{fmoil} \right)^{epoil} + \left(\frac{thinfac}{1 + vgcoef \cdot v_g^{vgexpn}} \right) + \left(\frac{fmcap}{N_C} \right)^{epcap} + \left(\frac{fmgcp - N_C}{fmgcp} \right)^{epgcp} \quad \textbf{(4.3)}$$

where in the F_1 function $\boldsymbol{W_S}$ is the surfactant concentration in the grid block, ***fmsurf*** is the critical surfactant concentration, ***epsurf*** is the parameter that controls the gas mobility's dependence on the surfactant concentration. In the F_2 function $\boldsymbol{S_w}$ is the water saturation in the grid block, ***fmdry*** is the critical water saturation and ***epdry*** regulates the slope of the relative permeability curve near the critical water saturation. In F_3 $\boldsymbol{S_o}$ is the oil saturation in the grid block, ***fmoil*** is the maximum oil saturation for stable foam and ***epoil*** is the parameter that decides the oil saturation's effect on the FM function. In the expression for F_4 $\boldsymbol{v_g}$ is the gas velocity, ***vgcoef*** is the gas velocity constant, ***thinfac*** is also a function constant, and ***vgexpn*** is the gas velocity exponent. In the functions F_5 and F_6 $\boldsymbol{N_c}$ is the capillary number, ***fmcap*** is the capillary number for reference foam, ***fmgcp*** is the critical capillary number for foam generation, and ***epcap*** and ***epgcp*** are exponents that control the capillary number's effect on the FM function. F_1 and F_2 are used in Paper 5-6, only F_1 is used in Paper 7.

In STARS foam is formed instantly everywhere gas, water and surfactant are present simultaneously. Vassenden et al. (1998[B]) found that foam propagated slower than the surfactant. It appeared that foam propagation was not limited by surfactant retention, but was delayed due to gravity segregation and presence of oil in the porous media.

4.2 Gravity segregation

When surfactant solution and gas or pre-generated foam is injected into a reservoir, the gas and liquid will eventually segregate into different flow path, see Figure 25. This segregation is caused by the fluids different density. It is favorable to increase the extension of the three phase area, the mixed flow zone. Increasing this zone will increase the sweep efficiency and thereby increase the oil recovery in the reservoir.

A useful model for gravity segregation is the Stone-Jenkins model, presented by Stone (1982) and further evaluated by Jenkins (1984). The model was first presented for uniform co-injection of gas and water in a homogeneous porous medium at steady-state. Stone assumed that in this case, fluid portioning in the reservoir is characterized by three regions of uniform saturation, with sharp boundaries between them, see Figure 25:

- a mixed zone with both gas and water flowing.
- an override zone with only gas flowing
- an underride zone with only water flowing

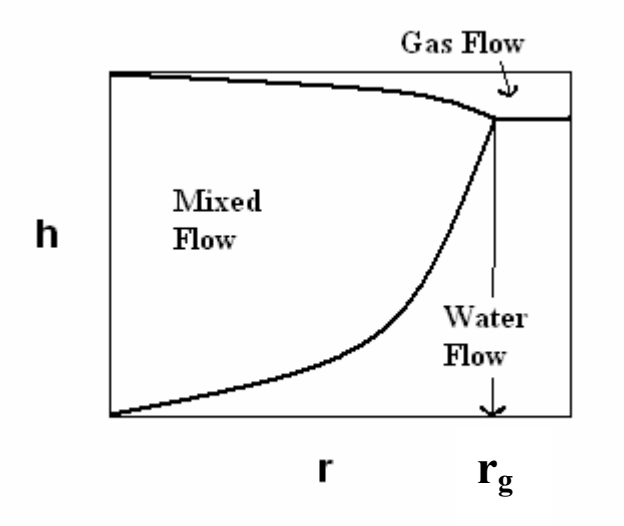

Figure 25: Schematic figure of the three zones in a cross-section of a foam flooded reservoir.

The assumptions for the Stone and Jenkins model are explained in further detail by Stone (1982) and Jenkins (1984). The Stone-Jenkins model gives us the dimensionless position, where gas and liquid flow completely segregates. The position is called the segregation length ($\mathbf{r_g}$ in a cylindrical reservoir and L_g in a rectangular reservoir). The formulas for a rectangular reservoir are presented elsewhere (Stone, 1982, Jenkins, 1984, Shi and Rossen, 1998). The formula for a cylindrical reservoir is given as:

$$\left(\frac{r_g}{r}\right)^2 = \frac{q_t}{k_z \cdot \Delta\rho \cdot a_H \cdot g \cdot \left(\frac{k_{rw}}{\mu_w} + \frac{k_{rg}}{\mu_g}\right)} \qquad \textbf{(4.4)}$$

where **r** is the outer radius of the reservoir, $\mathbf{q_t}$ is the total injection rate, $\mathbf{k_z}$ the permeability in vertical direction, **Δρ** the density difference between water/surfactant solution and gas, $\mathbf{a_H}$ the horizontal area between the wells, and **g** the gravity constant, 9,81 m/s^2. $\mathbf{k_{rg}}$ and $\mathbf{k_{rw}}$ are the relative permeability for gas and for water with the respective viscosities $\boldsymbol{\mu_g}$ and $\boldsymbol{\mu_w}$.

Later, Shi and Rossen (1998) have shown that the model also applies to foam displacements. For foam flow in a radial reservoir the equation is given below.

$$r_g = \sqrt{\frac{q_t \cdot f_w}{k_z \cdot \Delta\rho \cdot \pi \cdot g \cdot k_{rw}}} \qquad \textbf{(4.5)}$$

$\mathbf{f_w}$ is the water fractional flow in the foam

It has been shown that these equations fit simulations of gas-water flow over a wide range of parameter values, and even simulations of foam injection, in spite of the complexity of foam behavior (Shi and Rossen, 1998, Holt and Vassenden, 1996, 1997, Cheng et al., 2000). In two dimensional laboratory experiments the observed gas-water segregation was in good agreement with segregation theory, whereas foam segregation appears to be slower than predicted from theory (Holt and Vassenden, 1997). The 1 m sandpack experiments reported by Vassenden et al. (1998[B]) did not match the Stone-Jenkins model. In their 10 m sandpack the results were complex, therefore it was hard to say if the segregation was in line with theory.

Many simulations have been performed to investigate different foam models and injection strategies, especially for the Surfactant-Alternating-Gas (SAG) process (Shi

and Rossen, 1998[B], Shan and Rossen, 2004). Both these papers found that a SAG process at fixed injection pressure better controlled gravity override in homogenous reservoirs then either continuous injection of foam or a fixed-injection rate SAG process.

Stone (2004) proposed injection of liquid in an interval above gas in the injection well as a way to increase reservoir sweep. In Paper 5 and Paper 6 the effect of different injection strategies for foam is considered (Illustrated in Figure 26). The theory in Paper 6 is an extension of the work by Rossen and van Duijn (2004).

In addition to co-injection over the entire interval, the following strategies were used:

- Co-injection of gas and liquid over a portion of the interval,
- Injection of liquid above gas over the entire formation interval,
- Injection of liquid above gas in the bottom of the reservoir (Paper 5)
- Injection of liquid above gas in separate zones well separated from each other (Paper 6).

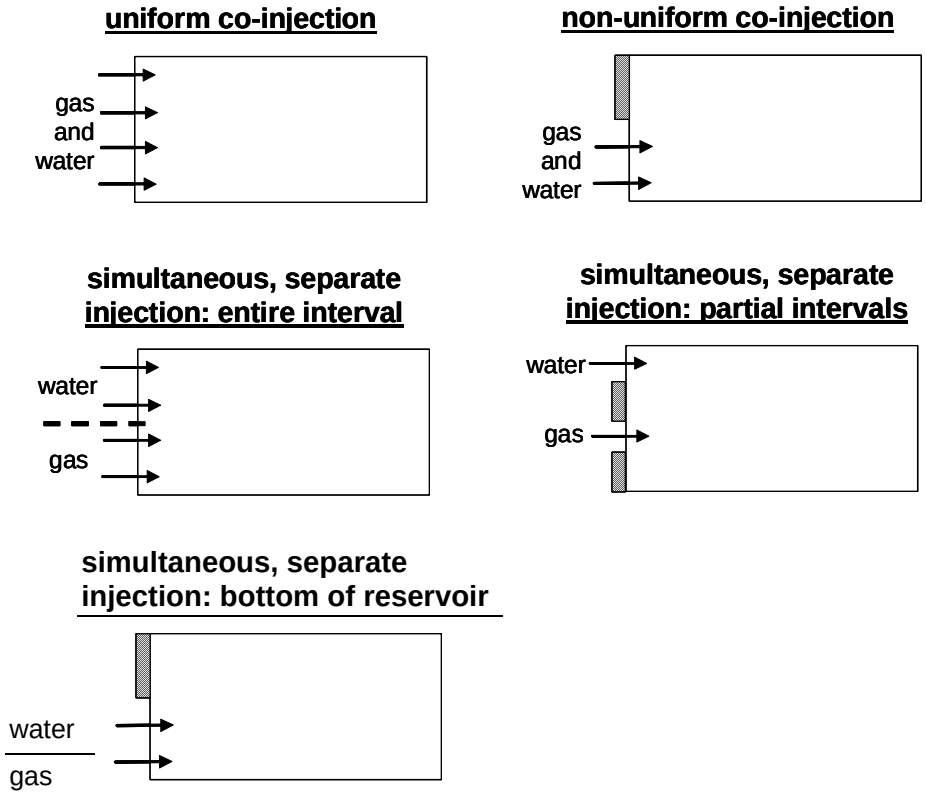

Figure 26: Schematic illustration of injection strategies considered in the simulations.

4.3 Field scale simulation

To try to predict the effect of the use of foam in an oil field, simulations and experimental work are important tools. Field scale simulations to estimate the foam potential on a field in the North Sea were performed using the STARS simulator from CMG. The details are presented in Paper 7. The production on the field started October 1 2003. Gas was observed earlier than expected in the production well P-1. A production well test was simulated to evaluate if foam had a potential for reducing gas inflow to this well. Foam potential for both a production well, and an injection well treatment were simulated in order to estimate any increase oil production and/or decrease in gas oil ratio (GOR).

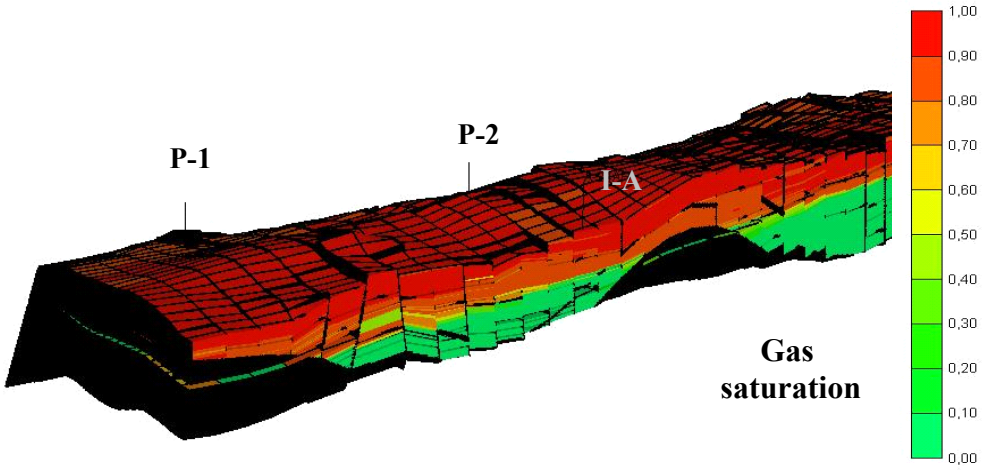

Figure 27: Illustration of the section of the field used in the simulations.

The generated history matched ECLIPSE files were used as the basis for the construction of the STARS files. The injection method and injection quantities chosen in the simulations are similar to that used in earlier simulation work (Surguchev et al., 1995, Aarra et al., 1996, Aarra and Skauge, 2000, Blaker et al., 2002, Skauge et al., 2002). The sensitivity to reservoir and foam properties was analyzed for a section of the reservoir (Figure 27). The segment consisted of two production well, P-1 and P-2, and one injection well, I-A.

Main results

We have used different experimental methods to investigate stability of foam, foam-oil interactions and foam propagation. A summary of our main findings will be presented in this chapter. Our main focus has been to investigate foam-oil interactions using static foam tests. We have investigated some of the main findings from these static experiments further in core flooding experiments at high pressure and temperature. We have also performed a simulation study of gravity segregation of foam in a small scale and simple model. An extended segregation length will increase the sweep efficiency and thereby improve the petroleum production. Finally, a foam potential study of a field in the North Sea was done. Simulations of a production well treatment, and an injection well treatment of a production-injector well pair, were performed.

5 Static foam tests

The results of the static foam experiments are reported in Paper 1-3. In Paper 1, static foam tests using alpha olefin sulfonate was performed to investigate foam-oil interactions. Experiments with variation in surfactant concentration, in amount of oil and in polarity of the oil phase were compared. In Paper 2 static foam tests using the fluorinated surfactant were compared to the alpha olefin sulfonate results. In Paper 3 results from static foam experiments for the two surfactants using a low surfactant concentration are compared. Experiments without oil and experiments varying amounts of alkanes as well as crude oil in both synthetic sea water and in 1wt% NaCl solution were performed. In addition, bulk solution properties for the two surfactants were measured to try to explain some of our findings.

5.1 Surfactant concentration

The surfactants are an alpha-olefin sulfonate (AOS) and a perfluoroalkyl betaine (FS-500). This study showed that foam was generated below cmc for both surfactants. The cmc was in the same range, 0,0022wt% for the AOS and 0,0028wt% for FS-500. Foam height increased with surfactant concentration. Both surfactants reached a constant maximum foam height at a certain concentration, 0,5wt% for AOS and

0,1wt% for FS-500 (Figure 28). AOS did show a multiple step increase in foam height. The foam column height did not change when the AOS concentration was increased from 0,01wt% to 0,1wt%. Nikolov et al. (1986) report that above a certain surfactant concentration after cmc, the stability of a foam increases sharply with surfactant concentration. An increased foam stability, at concentrations several times the cmc, is reported to be caused by the formation of a microstructure in the draining foam films (Wasan et al., 1994, Nikolov et al., 1986) The films will have a stepwise thinning process.

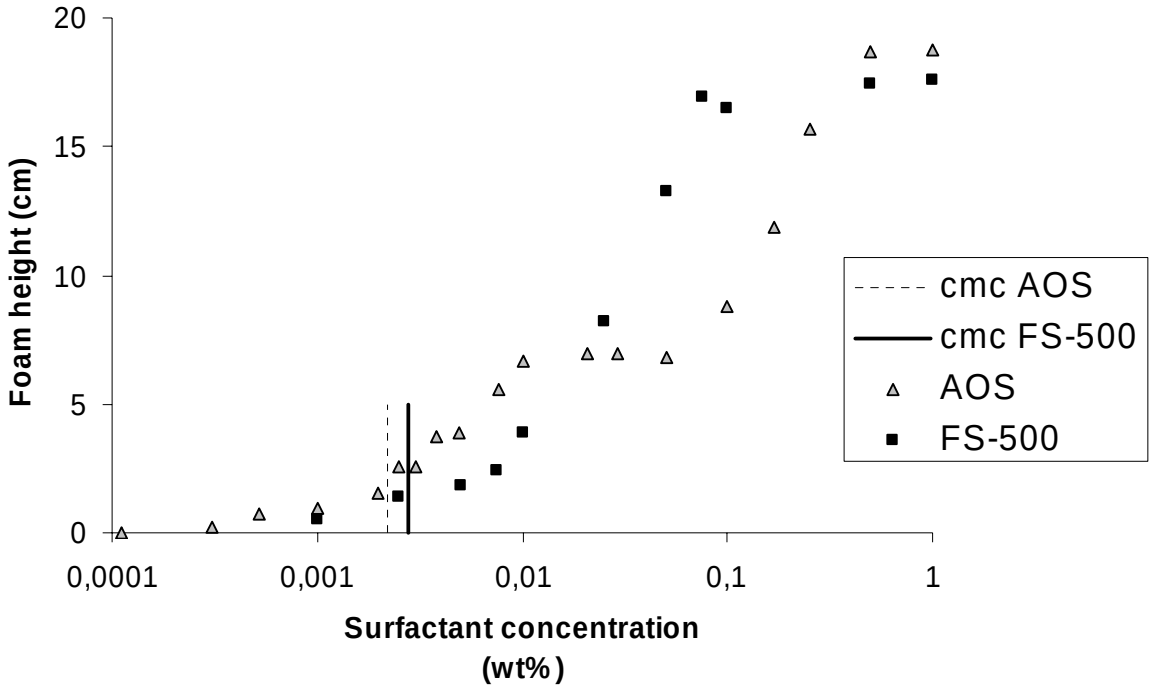

Figure 28: Foam height as a function of surfactant concentration for AOS and FS-500. Foam height was measured 4 hours after foam generation (Paper 2).

The literature suggests that with an increase in the concentration of the surfactant, a tendency can exist for surfactant micelles to change from spherical to cylindrical and then to lamellar structures (Kodama, 1973, Porte et al., 1984, Christian and Scamehorn, 1995). See Figure 2 in chapter 2. Abed et al. (2004) studied micellization of C_{12}-C_{18} alpha-olefin sulfonate. No transition from spherical to cylindrical micellar shape was observed for the experimental concentration range 0wt%-3wt%. They used

0-0,5wt% NaCl solution, a significant lower salt concentration than in seawater used in our experiments.

Viscosity measurements indicated a change in micelle structure close to the concentration for maximum foam height for each of the two surfactants (see Figure 29 for the AOS results and Figure 3 in Paper 3 for FS-500 results). The speed of sound results was different for the two surfactants, but both set of results indicated an abrupt change in speed of sound close to the concentration where the foam height increases. In the AOS system the cmc can be detected both by a sudden reduction in the speed of sound, and by a sudden change in the foam height. The fact that the slope of the speed of sound curve becomes more negative indicated a higher compressibility of the micellar state (Brun et al., 1978). For FS-500 neither the speed of sound nor the foam height changed significantly at the cmc.

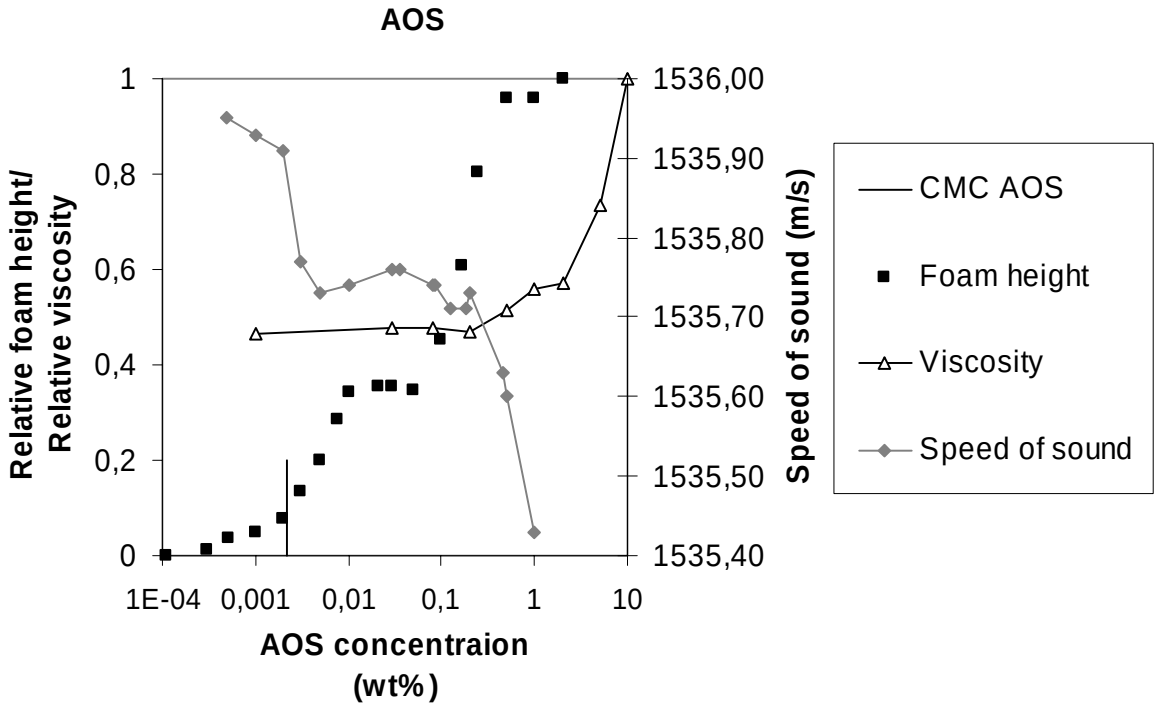

Figure 29: Relative foam height, relative viscosity and speed of sound measurements as a function of AOS concentrations. Foam heights were measured 4h after foam generation (Paper 3).

5.2 Alkanes

Short chain alkanes tended to destabilize foam, while long chain alkanes produced stable foam using 0,5wt% AOS and 1wt% alkane (Figure 30).

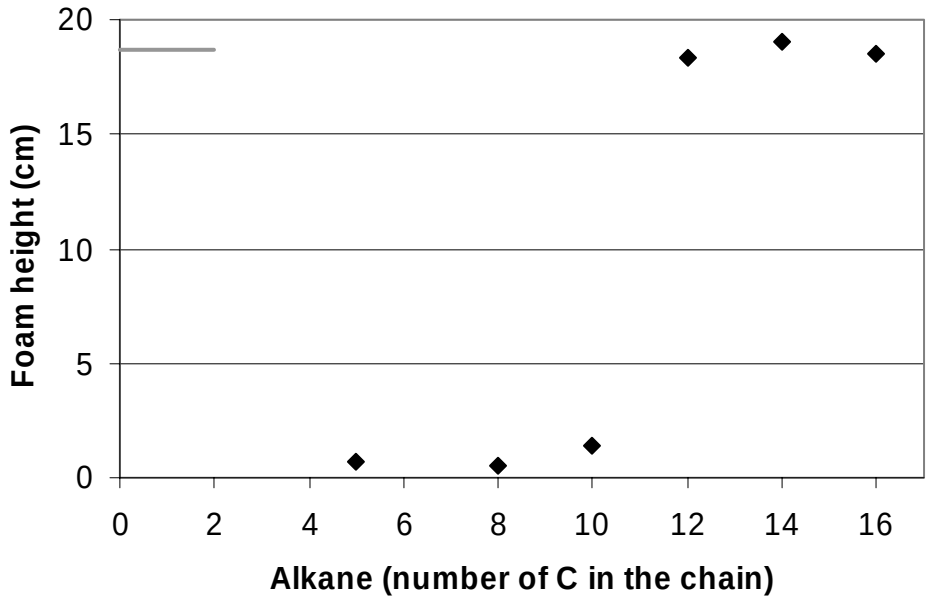

Figure 30: Foam column height after 4 hours for tests using 0,5wt% AOS surfactant and 1wt% alkane in synthetic sea water as a function of the number of carbons in the alkanes chain. The grey line indicates foam height in tests without oil (Paper 1 and Paper 2).

Similar results were reported by Suffridge et al. (1989) and Aveyard et al. (1993), as they found that lower molecular weight alkanes offered a more adverse environment to foam than alkanes with higher molecular weight in the surfactant systems they used. On the other hand Meling and Hanssen (1990) did not find any general correlation between destabilization of foam and oil molecular weight in the bulk foam tests and gas blockage tests they performed. Octane, dodecane and hexadecane were used in their experiments. Schramm and Novosad (1992) found a molecular weight dependent foam stability using crude oil, as foam stability in presence of crude oil decreased as molecular weight of the crude oil decreased. Kuhlman (1990) also found that a high concentration of light hydrocarbons in the oil destabilized the foam.

Using 0,1wt% AOS indicated similar results for the influence of alkane molecular weight as for foam test using 0,5wt% AOS (Figure 4 in Paper 3). The stability of foam using lower AOS surfactant concentration was poor.

Another interesting result was that it appeared that long chained alkanes produced more stable foam as compared to AOS without oil in brine. Arnaudov et al. (2000) and Denkov (2004) documented similar results for the surfactants they used. Draining of liquid films was slower with than without oil present. The Plateau borders were also thicker for the long chain alkanes than for the short ones. Foam Plateau borders for the short alkanes were visually similar to foam Plateau borders in tests without oil. Aveyard et al. (1993) also reported thicker lamellas in foam with added hexadecane than lamellas in foam with addition of shorter chain alkanes.

For 1wt% of alkane using FS-500, 17-18 cm foam was generated in every foam test using each of the different alkanes, which was similar to the foam height in foam tests without oil. For pentane the foam height was nearly twice the foam height seen with the other alkanes or in tests without oil. A reduction in the surfactant concentration from 0,5wt% to 0,1wt% did not seem to influence foam height for the FS-500 surfactant. Using 0,01wt% surfactant the foam height was reduced to 2-5 cm for the different alkanes.

Increasing the amount of alkane to 5 or 10wt% did not influence the foam height for foam testes using 0,5wt% AOS or FS-500. For AOS no oil phase between the liquid and foam columns were observed. All of the oil must therefore be in the foam structure, even for a 10wt% content of alkane. Dispersed oil droplets are often effective antifoam agents, but Koczo et al. (1992) found that emulsified oil increased the foam stability if the pseudo-emulsion film was stable, because oil drops in the Plateau borders inhibits the liquid drainage.

5.2.1 Solubilization

Adding a dye (Oil Red) to the alkane phase clearly showed the distribution of alkane between the foam and bulk brine phase. The dye itself did not affect the result as tests with and without the addition of dye gave equal results. Again, it appeared to be a difference between long versus short chained alkanes. For AOS decane and alkanes with shorter chain length are distributed both in the foam and in the bulk brine phase, thus, they have a higher ability to solubilize in the aggregates. The long chain alkanes did not color the brine phase, only the foam. This indicated that these molecules are not solubilized in the micelles. This variation in solubilization with alkane length is in line with solubility in water results summarized by McAuliffe (1979). For the fluorinated surfactant the change in solubilization is between C_5 and C_7. Pentane solubilized in the micelles, while heptane and longer alkanes did not. Foam stability in presence of oil seems to be related to transport properties within the foam for the AOS surfactant.

5.2.2 Spreading-, entering, and bridging-coefficient, and lamella number

Tables including all the spreading coefficients (S), entering coefficients (E), bridging coefficients (B), and lamella numbers (L) for the two surfactants using different combinations of alkane chain length and surfactant concentrations are presented in Paper 2 and Paper 3. All the values are equilibrium values. The lamella numbers are calculated using the simplified expression and assumptions presented in chapter 3.3.2. For the AOS surfactant the spreading coefficients are positive for all alkanes using 0,001wt% or 0,5wt% AOS. In foam tests, using 0,01wt% surfactant, spreading coefficient values are close to zero or slightly negative. The lamella numbers indicate moderately stable foam for all measured combinations, and the bridging coefficients are large and positive in most cases. The variation in foam stability for the AOS surfactant was neither reflected in the spreading coefficient values, nor for the other calculated parameters (E, L or B).

The spreading coefficients and lamella numbers were all indicating stable foam for all alkanes using FS-500. This was consistent with the static foam experiments using

0,5wt% or 0,01wt% surfactant, though for 0,001wt% surfactant the foam stability was poor.

The variation in spreading coefficients is mainly caused by the different surface tensions for the two surfactants. The surface tension for the AOS surfactant is 24 mN/m, and for FS-500 it is 14 mN/m. A lower surface tension for the surfactant will as indicated in the formula in chapter 3.3.1, reduce the spreading coefficient value.

The stability of the pseudo-emulsion film has not been measured in this study. It is therefore still open that pseudo-emulsions can play an important role in foam stability even for both surfactants. Koczo et al. (1992) and Lobo and Wasan (1993) found that the structure and stability of the pseudo-emulsion film was important for the foam stability in presence of oil in the foaming systems they investigated. The relationship between the spreading/entering coefficients and the foam stability is not general because it does not take into account the properties of the pseudo-emulsion film (Koczo et al., 1992).

5.3 Effect of alcohol and oil polarity

Foam tests using methanol generated 18-20 cm foam and experiments using octanol generated about 0,5 cm foam for both surfactants. The FS-500 was stable for all concentrations of butanol, while AOS foam was only stable using butanol concentrations less than 5wt%.

The foam height was reduced from 17,5 cm in foam tests without oil to 2-4,5 cm foam in tests using xylene or toluen. The result was similar for both surfactants. Based on these studies, it is difficult to make a general conclusion regarding the influence of oil polarity on foam stability.

5.4 Crude oil

The 9 different crude oils used in this study, denoted oil a-i, were obtained from North Sea oil reservoirs. Oil g, h, i are denoted oil 1, 2, 3 respectively in Paper 4. For the AOS surfactant the crude oils showed different abilities in destabilizing the foam in experiments using 0,5wt% AOS and 1wt% crude oil (Figure 31). For the crude oils that generated stable foam, oil b, d-f and h, the foam heights were 13-20 cm after 4 hours. The foam heights were only 1cm after 4 hours for the other crude oils (Figure 31). Reducing the AOS concentration to 0,1wt% decreased the foam height from 13-20 cm to 1cm in foam tests using the stable crude oils b, d-f and h. Two examples are shown in Figure 5 in Paper 3.

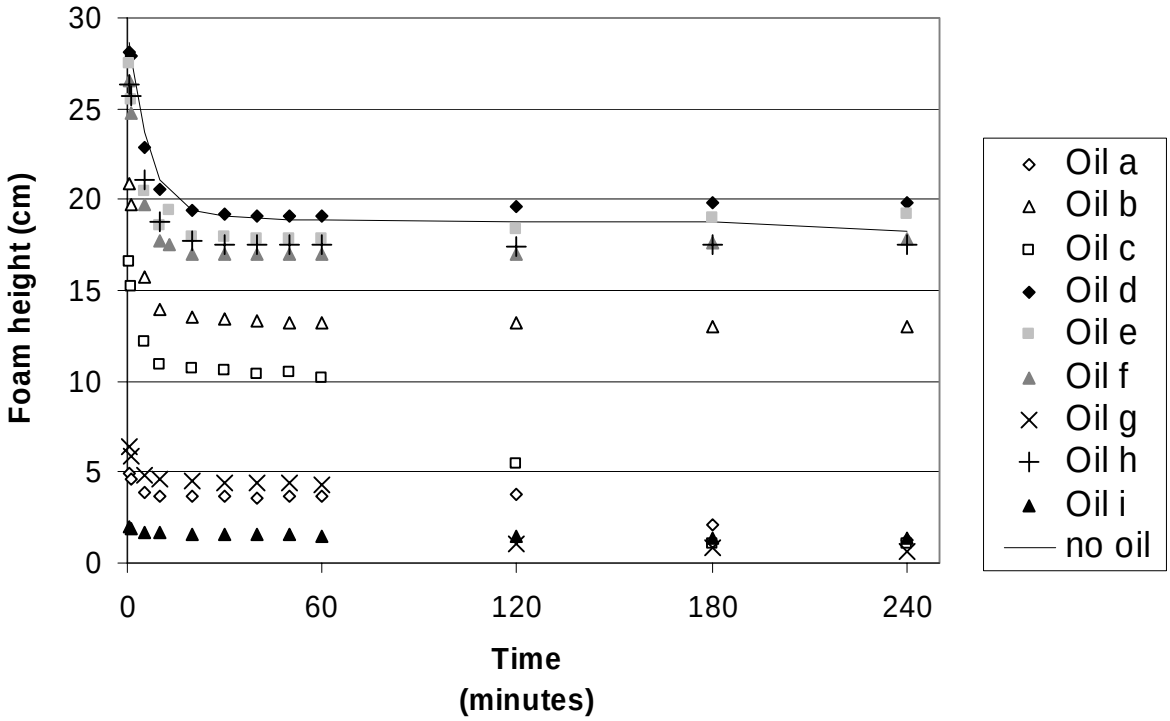

Figure 31: The plot shows foam column height as a function of time for the different crude oils using 1wt% oil and 0,5wt% AOS in synthetic sea water.

A multivariate data analyzes were performed to try to explain why some crude oils destabilized the foam while others generated foams that were stable in presence of oil in foam tests using 0,5wt% AOS. Physical and chemical properties including acid and base number, paraffin and asphaltene content, interfacial tension, spreading coefficient, viscosity, and foam column height for oil a-f were included in the

analyzes. (Density, viscosity, and interfacial tension for the crude oils were measured, and the spreading coefficient was calculated. Asphaltene and paraffin content, and acid and base number are reported by Skauge et al. (1999)). The influence of the physical and chemical properties is complex, and no direct correlation to foam stability was found. No single value was found to explain the complex foam-oil interactions observed.

Static foam experiments were also done using 5wt% of crude oil in 0,5wt% AOS in synthetic sea water. In these experiments, the foam height was 2-5 cm for all the crude oils (Figure 7 in Paper 1). Using 1wt% NaCl instead of synthetic sea water in similar tests with 5wt% of crude oil increased the foam stability for some of the crude oils. A similar result as for 1wt% of crude oil in synthetic sea water was obtained. These experiments show that a reduced ionic strength increased foam stability in the presence of oil for the AOS surfactant.

The stability of the foam was similar for all the crude oils in foam tests using 0,5wt% FS-500. The foam height was stable for more than a week. The foam heights were 16-18 cm for 0,5wt% and equal for 0,1wt% surfactant. Reducing the surfactant concentration to 0,01wt%, the foam was still stable for all oils, but the foam heights were only 1-3 cm.

5.4.1 Foam texture

The foam texture and oil configuration in foam were very different for the stable and moderately stable crude oils using the AOS surfactant. Crude oil b and d generated stable foam with thick oil filled liquid films (Figure 32). The foam height was stable for 2-3 days for these crude oils.

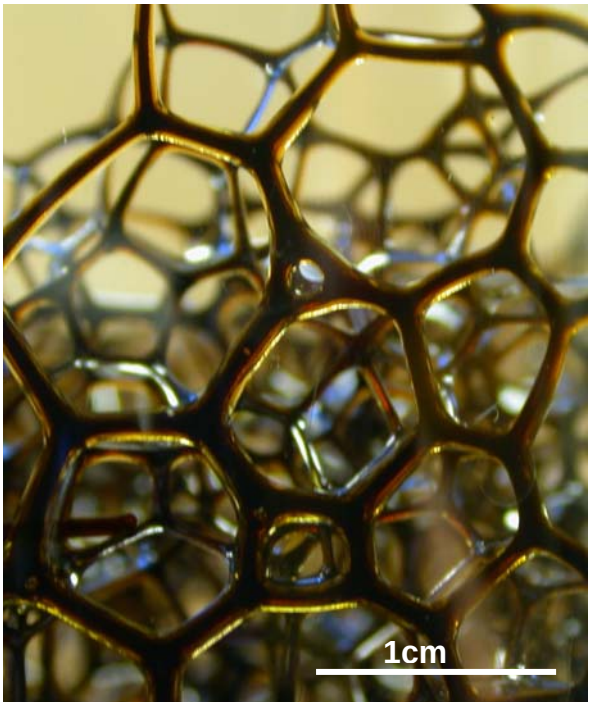

Figure 32: The picture shows foam with abundant oil in the Plateau borders. The foam is from a foam test using 1wt% of oil b and 0,5wt% AOS in synthetic sea water. The picture is taken 24 hours after mixing and is enlarged 3 times.

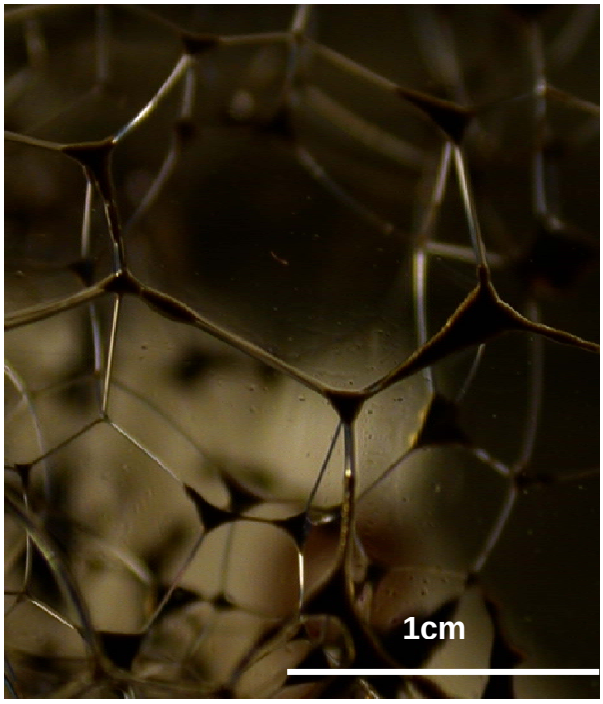

Figure 33: The picture show foam with thin Plateau borders and oil in the junction of the Plateau borders. The foam is from a foam test using 5wt% of oil e and 0,5wt% AOS in synthetic seawater. The picture is taken 24 hours after mixing and it is 4 times enlarges.

Foam stability for oil e-f and h was relatively stable for some hours using AOS, but the foam was almost completely broken down after 1 day. In these tests most of the oil drained out of the foam, and left oil in the Plateau border wedges during the first hours (Figure 33). The Plateau borders in these tests were thin.

Visually, the FS-500 foam (Figure 34) had a denser bubble concentration than the AOS foam. It was also significantly more stable over time than the AOS foam. Foam tests using the FS-500 surfactant could be stable for weeks. Figure 35 shows that the

oil is present as droplets in the lamellas. During the process of foam lamella thinning, the oil droplets are left in the Plateau borders, as indicated in Figure 34.

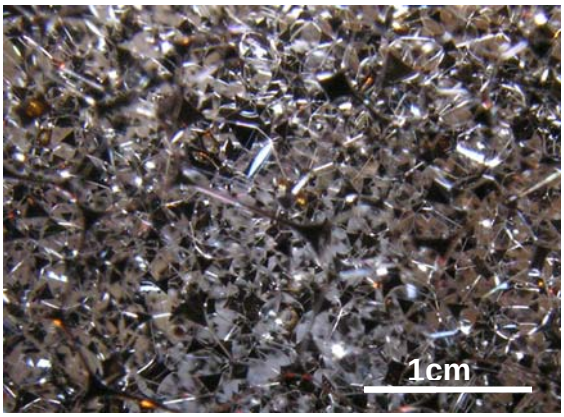

Figure 34: 1wt% of crude oil I in synthetic sea water using 0,5wt% fluorinated surfactant. The picture is taken one day after mixing.

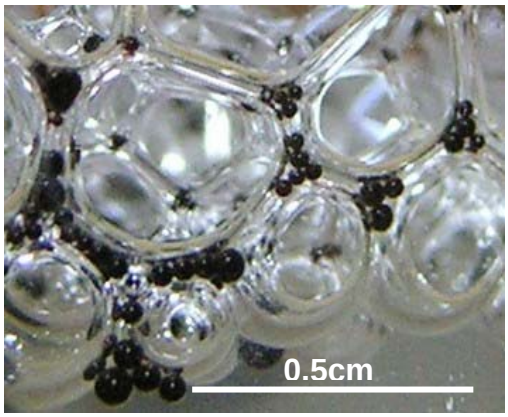

Figure 35: Static foam experiment using 1wt% crude oil i and 0,5wt% FS-500 in synthetic sea water. The crude oil forms droplets in the Plateau borders. The picture is taken a few hours after mixing.

5.4.2 Spreading-, entering-, and bridging-coefficient, and lamella number

The spreading coefficient, entering coefficient, lamella number and bridging coefficient for all the crude oils are presented in Table 1 for the AOS surfactant, and in Table 2 for the FS-500.

Table 1: Spreading coefficients, entering coefficients, lamella numbers and bridging coefficients at equilibrium for the AOS surfactant.

Crude oil	Spreading coefficient	Entering coefficient	Lamella number	Bridging coefficient
Oil a	11,1	11,9	10,4	489
Oil b	4,6	5,6	8,1	250
Oil c	4,2	5,6	5,8	241
Oil d	7,3	7,9	12,3	353
Oil e	5,4	9,0	2,3	340
Oil f	4,7	7,9	2,5	303
Oil g	-3,2	-0,4	2,5	-85
Oil h	-0,2	0,6	11,6	13
Oil i	-5,9	-5,0	9,5	-337

All the coefficients for the AOS are positive for most of the crude oils and the lamella number indicate moderately or low stability foam. The spreading coefficients are negative for oil g and oil i, and also slightly negative for oil h. The entering- and bridging coefficient also indicate stable foam for oil g and oil i. Oil b and oil d-g generated stable foam. It is therefore a lack of correlation between the calculated values in Table 1 and static foam stability.

Table 2: Spreading coefficients, entering coefficients, lamella numbers and bridging coefficients at equilibrium for the FS-500 surfactant.

Crude oil	Spreading coefficient	Entering coefficient	Lamella number	Bridging coefficient
Oil a	-2,7	6,7	0,4	72
Oil b	-8,3	-1,7	0,7	-164
Oil c	-8,9	-2,9	0,8	-204
Oil d	-4,8	8,0	0,3	84
Oil e	-8,4	2,0	0,5	-88
Oil f	-6,3	3,1	0,5	-29
Oil g	-15,0	-5,4	0,5	-403
Oil h	-14,8	-7,6	0,7	-477
Oil i	-21,9	-10,1	0,4	-776

For the fluorinated surfactant all the calculated spreading coefficients and lamella numbers indicated stable foam in accordance with theory. Two of the crude oils have positive bridging coefficient. This is a necessary, but not sufficient, criterion for the foam to behave as an antifoaming agent. Four of the entering coefficients are positive; this indicates that these oils may enter the surface of the lamellas. There is no indication that these oils generate less stable foam in the static foam experiments than the other oils.

6 Core flooding

The results from the core flooding experiments are presented in Paper 4. The results from core flooding experiments were compared to results from static foam tests (Paper 1-3). The role of similarity or lack thereof between static and dynamic foam tests is a subject of ongoing debate in the literature.

6.1 Core flooding experiments without oil

In experiments without oil AOS and FS-500 generated foam with similar strength, both in the static foam tests and in the dynamic foam experiments. The propagation rate was also approximately equal for the two surfactants in the core flooding experiments without oil (Figure 2 in Paper 4). The differential pressure (dP) in the last part of the core was about 1,5 times higher than in the first part of the core, indicating generation of even stronger foam. This is consistent with core flooding experiments performed by Mannhardt and Svorstøl (1999, 2001) and Mannhardt et al. (2000).

6.2 Core flooding experiments with residual oil

In Paper 4 we have examined foam generation capability for an alpha olefin sulfonate and a fluorinated surfactant in cores with residual oil saturation. First we wanted to compare dynamic foam properties for the oils decane and hexadecane since the static foam properties were quite different for these oils using the AOS surfactant. Unfortunately, these model oils tended to block the core in some way. Flooding experiments through 10 μm and 5 μm metal filters indicated similar blocking effect. In both the core and filter experiments the differential pressure increase rapidly, and reached a high pressure level in short time. The blocking might be caused by emulsion formation. Gel like particles were observed, but foam was never observed in the visual cell during the experiments.

Because alkanes caused blocking problems, we continued the flooding study using three crude oils, oil g, h, i (Oil 1, 2, 3 in Paper 4). The main disadvantage of using crude oils is their complex composition compared to model oils. This makes it more

difficult to identify composition parameters and oil properties that are important for stable foam generation. On the other hand using crude oil is closer to real application than simple alkane oils. No tendency to block the core was observed in any of these experiments.

6.2.1 Foam strength

Foam strength seemed to be independent of presence of oil in the core flooding experiments using FS-500 (Figure 36). Consistent with results observed in the static foam tests. AOS generated foam with differing foam strength for the different crude oils in the core flooding experiments. The correlation between the static and dynamic foam experiments was poor for the AOS.

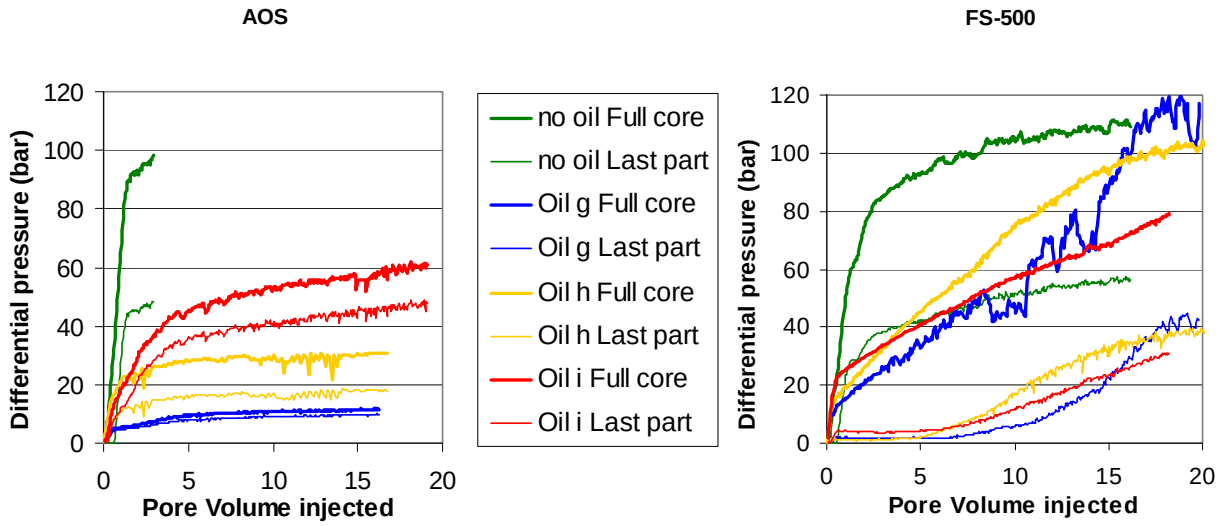

Figure 36: Differential pressure as a function of pore volume injected fluid for the core flooding experiments using AOS (left plot), and FS-500 (right plot). The thicker line presents the total core dP, and the thinner line presents dP over the last part of the core (Paper 4).

In the core flooding experiments with oil, FS-500 generated foam that has equal foam strength throughout the core or stronger foam in the first part of the core (Table 4 in Paper 4). The AOS surfactant again showed stronger foam in the last part of the core, similar to the experiment without oil.

6.2.2 Foam propagation

Foam propagation rate was influenced by residual oil saturation. AOS surfactant showed a faster propagation rate in comparison to the propagation rate with the FS-500 surfactant, which was significantly delayed in the presence of S_{orw} (Figure 37).

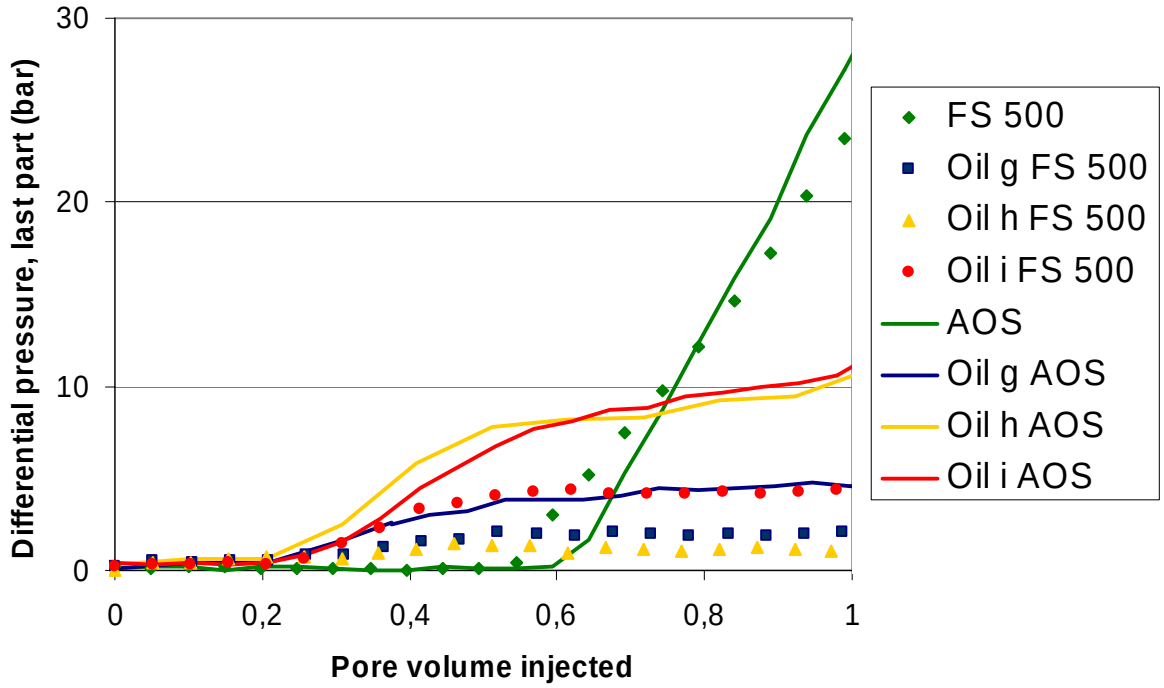

Figure 37: Differential pressure as a function of pore volume injected fluid for the pressure tab located 17,8 cm from the inlet end of the core (Paper 4).

6.3 Foam texture in the visual cell

The visual cell at the outlet of the core was used to indicate the presence of foam in an experiment. Further, it was used to observe the time needed for the foam to propagate through the whole core. In experiments without oil foam was observed in the visual cell after about 2 hours for both surfactants. Using AOS surfactant and residual crude oil, foam was observed after approximately equal time as without oil, while it took more than 20 hours for foam to propagate through the whole core using the FS-500. In experiments without oil it is almost impossible to see the foam bubbles in the viewing glass, because the foam is so dense (Figure 38). Figure 39 shows one example of a core flooding experiment with crude oil present. The foam is usually light brown, and

it is possible to see the bubbles. The two surfactants generate foams that were visually similar both with and without oil.

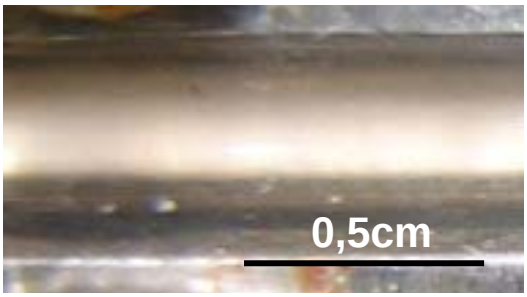

Figure 38: FS-500 reference foam in the visual cell during the core flooding experiment

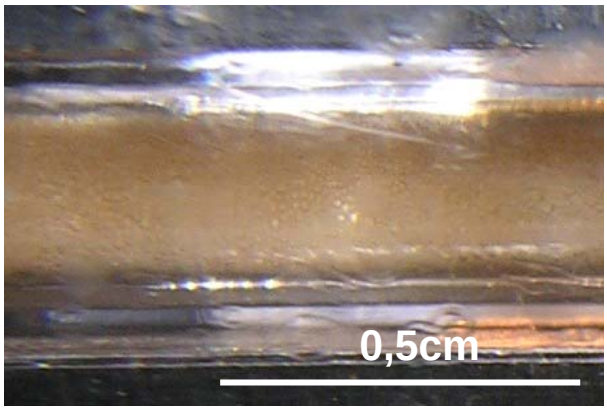

Figure 39: Foam in the visual cell during the core flooding experiment using oil g and AOS.

7 Simulation

7.1 Gravity segregation

The gravity segregation study is presented in Paper 5 and Paper 6. In Paper 5 several reservoir parameters and foam properties have been varied to test the different injection methods (Figure 24 in chapter 4). These parameters are the reservoir size, the ratio between the horizontal and vertical permeability, the mobility reduction factor and other foam parameters in STARS. In some experiments the foam quality and the permeability in the horizontal direction were also varied. The simulations in Paper 5 show that the segregation length is almost identical for the four injection methods, when all other parameters including injection rate are fixed. However, the segregation length apparently increased somewhat as water was injected in the upper half reservoir and gas in the bottom half reservoir. The shape of the foam bank is different for the four injection methods for simulations with foam. In this way the total area swept by foam may vary for the different injection strategies.

When comparing the simulation results to the Stone-Jenkins model (Stone, 1982, Jenkins, 1984), there is a quite good match for the segregation length of foam. The original Stone-Jenkins model, as described in chapter 4, is derived for uniform co-injection of water and gas. The model was later modified to fit uniform foam injection (Shi and Rossen, 1998). Even if the model is derived for uniform injection, apparently it can be used for other non-uniform injection methods as well.

The reservoir in Paper 6 is 20 m thick and has a radius of 120 m. One of the reservoirs sizes used in Paper 5 has similar reservoir size, but the number of grids is significantly larger in Paper 6 than in Paper 5. In Paper 5, we used only 500 grid blocks, but in Paper 6, the number of grid blocks was 3200. This improved our results.

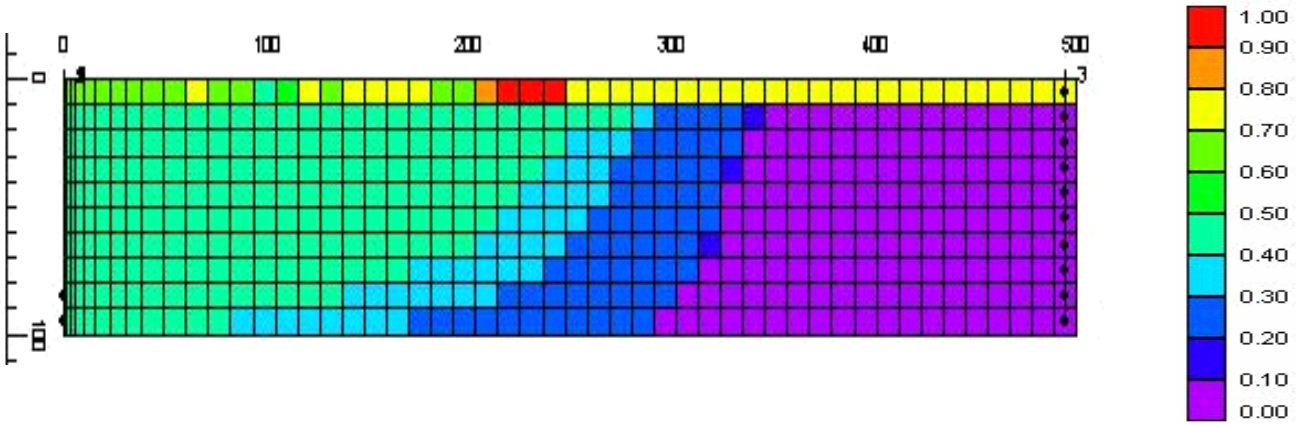

Figure 40: Example of the simulation model in Paper 5. The figure shows the gas saturation, the size is given in ft. The boundary of the foam bank is not sharp.

Because of the improvements of the numerical dispersion in Paper 6, the foam bank boundaries are sharper (compare Figure 40 and Figure 41-Figure 44). The conclusion is also somewhat different. There is little or no change in segregation length at fixed injection rate, in the case of uniform injection and only injection in a restricted interval. This is true for both co-injecting fluids and injecting water above gas. The volume of reservoir swept by gas may be affected by these different injection strategies, as found in our earlier study as well (Paper 5). At fixed total injection rate, injection of water above gas gives deeper penetration before complete segregation than co-injection does, but again, exactly where the two fluids are injected does not affect the segregation length. Stone (2004) also found that simultaneous injection of gas and water, injecting gas low in the formation and injecting water in a separate site above, improved the gravity segregation length. Figure 41-Figure 44 presents one set of simulations using the different injection strategies. The injector is located to the left and the producer to the right.

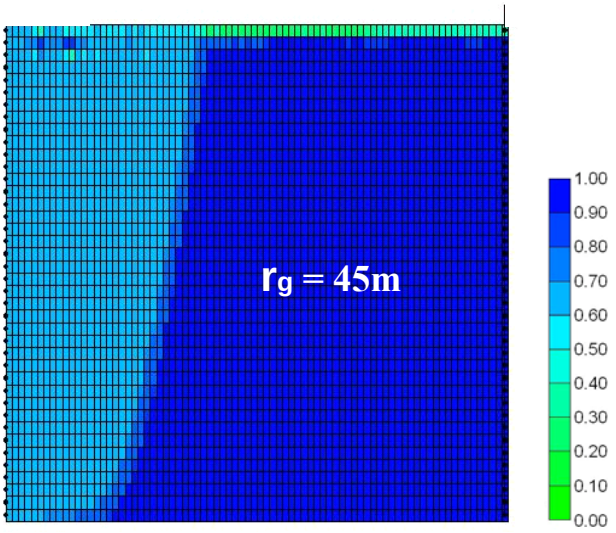

Figure 41: Steady-state water saturation for uniform co-injection of gas and liquid (foam) along the entire vertical interval. Gravity segregation occurs 45 m from the injection well.

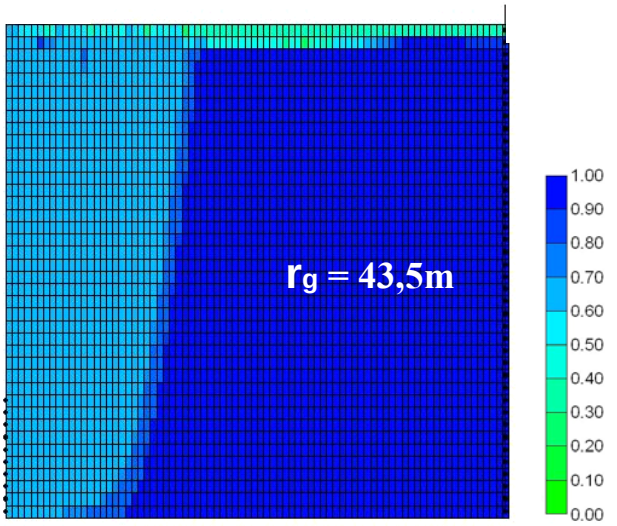

Figure 42: Steady-state water saturation for co-injection of gas and liquid (foam) in the bottom 5 m (10 grid blocks) of the vertical interval. Gravity segregation occurs 43,5 m from the injection well.

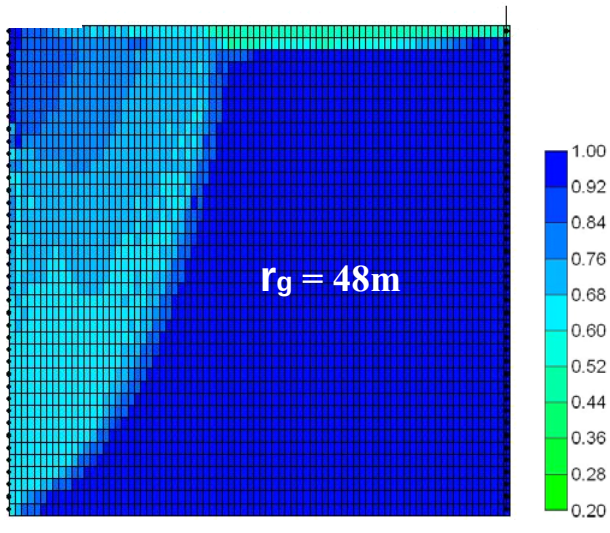

Figure 43: Steady-state water saturation for injection of gas in the bottom 15 m and liquid in the top 5 m of the vertical interval. Gravity segregation occurs 48 m from the injection well.

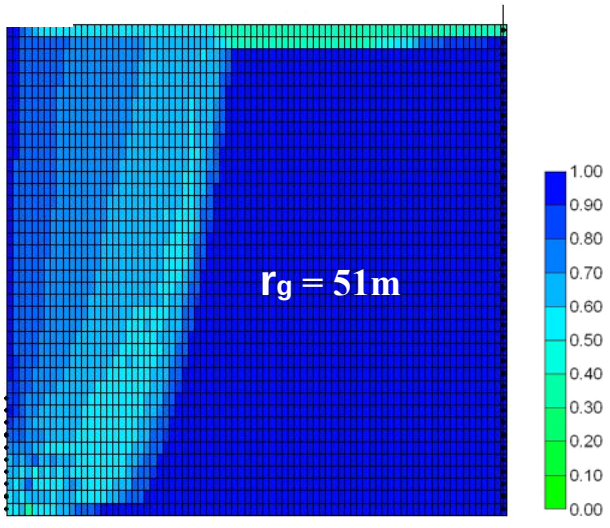

Figure 44: Steady-state water saturation for injection of gas in the bottom 3,5 m of the vertical interval and liquid in the 1,5 m immediately above this. Gravity segregation occurs 51 m from the injection well.

The best strategy to improve sweep efficiency if injection pressure is limited is to use the entire formation height for injection. Injection of water in an interval above gas, where the intervals are chosen to minimize injection well pressure, will therefore be the optimal injection strategy. Shi and Rossen (1998[B]), and Shan and Rossen (2004),

found that fixed injection pressure better controlled gravity override in homogenous reservoirs than either continuous injection of foam, or a fixed-injection rate for the SAG process.

The gravity segregation model presented by Rossen and van Duijn (2004) has been further developed and improved in Paper 6. The computer simulations described above, confirm the predictions of the theory. The distance to the point of segregation in every case is within 3 m, of that predicted by theory.

7.2 Field scale simulation

In Paper 7 the foam potential for a production well and an injection well treatment for a North Sea reservoir are presented. A history matched eclipse simulation model was converted to the STARS simulation model used in the foam potential study. All the details for the simulation setup and injection methods are described in the paper. Injection methods and foam properties are similar to methods and properties in earlier field tests (Surguchev et al., 1995, Aarra et al., 1996, 2002, Blaker et al., 2002, Skauge et al., 2002). Only the mobility reduction factor was varied in the sensitivity study. The no foam case represents a scenario in which equal amount of water as surfactant solution is injected, and the two cases have equally amounts of gas injected.

Production well

Simulations of production well treatment of well P-1 showed a significant reduction in gas oil ratio for the foam cases. Using cycles of two days of surfactant injection, and one day of gas injection, the gas inflow to the well was delayed for 1-4 months dependent on the mobility reduction factor (MRF), see Figure 46. MRF values between 10 and 300 were used in the simulations. During the simulation period May 1 2005 to June 5 2008 the cumulative oil production was increased by $34 \cdot 10^3$ Sm^3 (Figure 45), and the gas storage potential was $7{,}04 \cdot 10^7$ Sm^3 for the foam case using MRF 100. In the simulations for the production well treatment in the Oseberg

field the foam was estimated to delay gas breakthrough by 50-100 days, and to increase the oil production by 21-100·10^3 tons (Aarra et al., 1996)

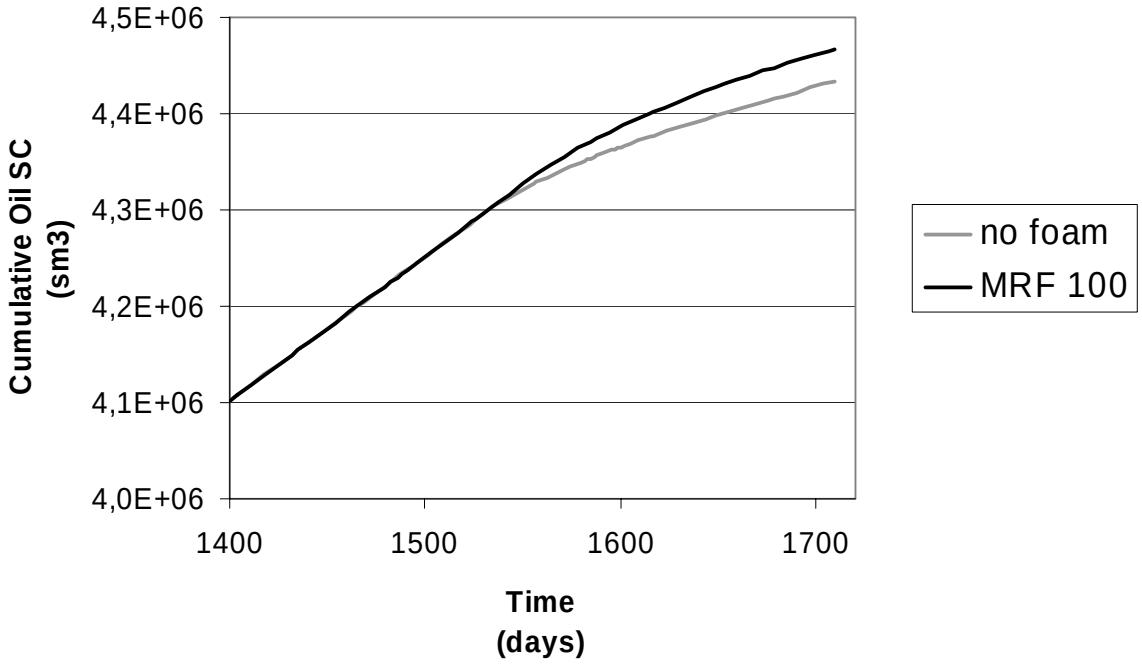

Figure 45: Cumulative oil production for the no foam and MRF 100 cases for the production well treatment as a function of time (Paper 7).

When increasing the injection period 7 times, the increased injection volume of surfactant showed improved foam performance. Using this injection period of 2 weeks for the surfactant, and 1 week for the gas showed that the gas oil ratio was reduced for 6 months compared to a no foam case (Figure 46).

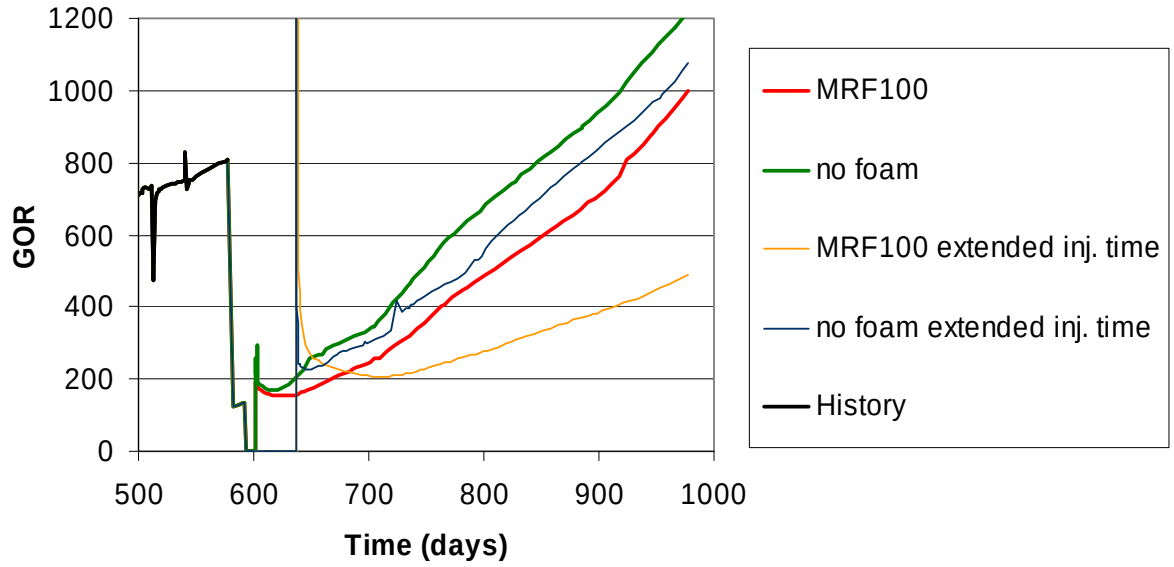

Figure 46: Gas oil ratio as a function of time using different MRF values in the production well treatment

Injection well

Injection well treatment simulations of well pair P-2 and I-A were performed. The simulations showed an increase in gas storage potential and increased oil recovery, in the range of 155 kSm^3 for simulations using MRF 100 compared to the no foam simulation case (Figure 47). Similar gas storage potential and oil recovery potential were reported by Aarra et al. (2002). Unfortunately, the increased oil production is significantly delayed, and this complicates the evaluation of the results.

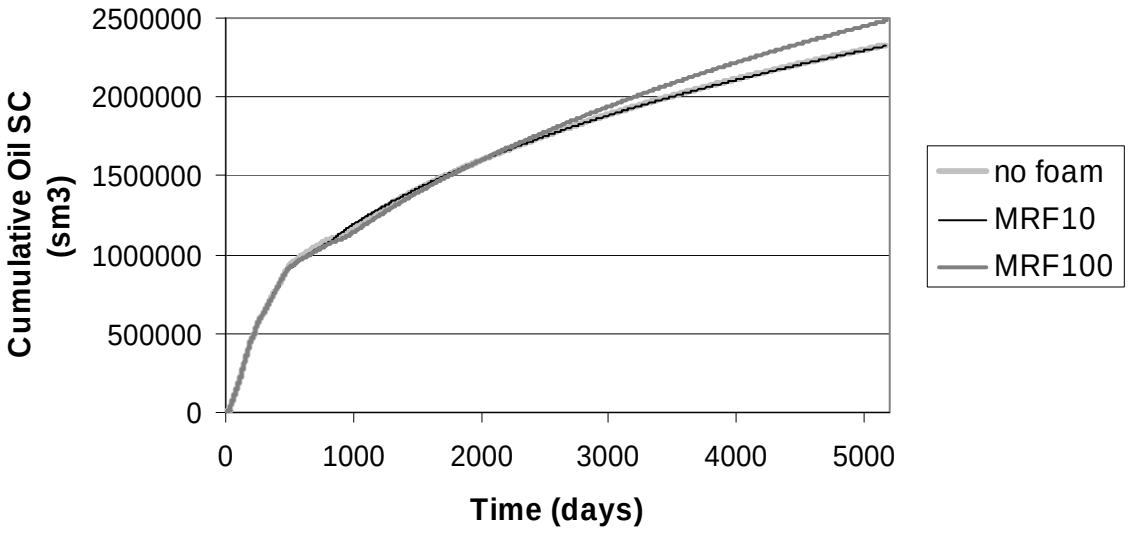

Figure 47: Cumulative oil production for the no foam, MRF 10, and MRF 100 cases for the injection well treatment as a function of time (Paper 7).

8 Summary

The results of these experimental studies show that foam is generated below cmc for both the alpha olefin sulfonate and the FS-500 surfactant. Even in experiments using an addition of oil, foam is generated below the cmc concentration, but the stability was poor in these tests. In experiments without oil foam height increased with increasing surfactant concentration for both surfactants, but AOS did show a multiple step increase in foam height. Both surfactants reached a constant maximum foam height at 0,1-0,5wt%, and this might be related to the bulk micelle structure. Changes in ionic strength and composition did not affect the foam height in experiments without oil. For the AOS surfactant a reduced ionic strength increased foam stability in the presence of oil.

We found that solubilization was an important mechanism for the stability of foam in presence of alkanes. The limit for solubilization was different for the two surfactants. Using AOS, decane and alkanes with lower molecular weight were solubilized in the micelles, and these light alkanes broke or destabilized the foam. Using FS-500, pentane was solubilized, but alkanes with higher molecular weight were not. Foam tests using pentane gave significantly more foam than using other alkanes.

Foam can be stable in presence of oil using both surfactants, but FS-500 generated more stable foam than AOS in presence of oil, both in static and core flooding experiments. The crude oils showed different abilities in destabilizing the foam in experiments using AOS, while FS-500 generated stable foam in all static tests in presence of oil. A multivariate data analyzes was performed for the AOS surfactant results from the bulk foam tests using addition of different crude oils. Physical and chemical properties for the different crude oils were included in the analyzes. No single parameter or property could explain the complex interactions observed in the static foam tests.

Foam was generated in all core flooding experiments with and without oil for both surfactants. The AOS generated foam with varying foam strength for the different

crude oils in the core flooding experiments. The correlation between the static and dynamic experiments was poor for this surfactant. The strength of the FS-500 foam was similar in core flooding experiments with and without oil. This is consistent with the FS-500 results from the static foam tests. Foam propagation rate was influenced by residual oil saturation. AOS generated weaker foam than the FS-500, but the propagation rate was more rapid for the AOS in presence of residual oil saturation (S_{orw}). From observations in a visual cell and pressure measurements the AOS surfactant showed a faster propagation rate in comparison to the propagation rate using the FS-500 surfactant, which was significantly delayed in the presence of residual oil saturation. The surfactants generated foam with similar strength and propagation rate in core flooding experiments without oil.

In general spreading, entering, and bridging coefficients and the lamella numbers indicated stable foam with the FS-500 and destabilization of foam with the AOS surfactant. In spite of this several static and all dynamic foam tests using AOS generated stable foam. The variation in spreading coefficient is mainly caused by the different surface tension for the two surfactants. The stability of the pseudo-emulsion film has not been measured in this study. It is therefore still open that pseudo-emulsions can play an important role in foam stability even for both surfactants.

At fixed total injection rate, injection of water above gas gave an increased segregation length compared to co-injection. Whether the fluids were uniformly injected over all or any portion of the formation interval did not affect the segregation length. When injection pressure is fixed, the predicted benefit from injection of water above gas is significant greater than using fixed injection rate. The simulations showed a significant effect of numerical dispersion.

Simulations of a production well treatment showed a significant reduction in gas oil ratio using foam injection. The oil production was also increased. The complex reservoir properties complicated the evaluation of the injection well treatment results. Gas storage potential and oil recovery were increased, but were significantly delayed.

9 Further work

In this study we have investigated foam and especially foam-oil interactions. Various experiments and simulations have been done and the results examined. The different experimental methods have been performed to do a systematic investigation of foam and foam-oil interactions. The goal of this study has been to try to elucidate and improve the understanding of foam and to try to identify possible correlations between static and dynamic foam properties. Our results have shown that correlation between static and dynamic properties is complex, and further investigation is needed. It was difficult to find any direct correlation between static and dynamic foam tests for the AOS surfactant. More experiments using a larger variation in foam and oil parameters may improve understanding this correlation.

Two surfactants have been used in this study. The FS-500 seems to be more tolerant to oil and produces stable foam at lower surfactant concentration than the AOS. What mechanisms makes FS-500 a more stable surfactant than the AOS surfactant? The surfactant surface tension seems to be important for foam stability. Can further measurements of the physical or chemical foam and oil properties improve our understanding of foam-oil interactions? Some of the foam properties are measured for static conditions; it would therefore be interesting to investigate properties like the dynamic surface or interfacial tension.

A further study of the oil configuration in the foam films may also improve our understanding of foam-oil stability. Our experimental results indicate that it is difficult to find any general correlation between foam stability and the spreading coefficient, entering coefficient, lamella number or bridging coefficient theory. Solubility and solubilization seems to be an important factor, especially for the AOS surfactant. Measurement of solubility and solubilization in the two surfactant systems is therefore one area of interest. Is the solubility determining for the foam stability and can other theories, like the pseudo-emulsion film give an explanation? Stability of the pseudo-emulsion film has been suggested to be important, so to try to identify this mechanism in our systems may be important.

A few suggestions to further investigate the challenges described here and to improve our understanding of foam are given below.

In this study 9 different crude oils were used in our static experiments, and 3 of them were used in the dynamic core flooding experiments. These oils have different composition, physical and chemical properties. Increasing the number of crude oils in the data set will give a larger amount of results, and this might give a better understanding of the foam-oil interaction mechanisms. The large amount of data may be analyzed by multivariate data analyzes or other methods to try to identify important oil properties for predicting foam stability.

Our static foam experiments, in Paper 1-Paper 3, have produced many interesting results. In Paper 3 we present static foam experiments using low surfactant concentrations. It was found that the FS-500 generated stable foam at a lower surfactant concentration than the AOS. Results also show that reducing the FS-500 surfactant concentration from 0,5wt% to 0,1wt% did not influence the foam stability. All the core flooding experiments in Paper 4 are performed at a surfactant concentration of 0,5wt%. To perform core flooding experiments as a function of surfactant concentration may indicate how important the surfactant concentration is for foam stability, and for the foam-oil interactions in dynamic experiments.

The core flooding experiments presented in Paper 4 showed that the AOS generated weaker foam than the FS-500, and the propagation rate was more rapid for the AOS in presence of residual oil saturation after water flooding. It would therefore be interesting to investigate the residual oil saturation after foam flooding in the cores used in these experiments. Especially it would be interesting to see if the oil saturation is different for cores from experiments using AOS and cores from experiments using FS-500. We would also like to compare foam propagation and foam generation in the core flooding experiments to the residual oil saturation along the cores.

Experiments using polymer enhanced foam is a topic of interest. Earlier work has shown that addition of polymer to water continuous foam can improve gas-blocking ability. Core flooding experiments performance using polymers may be compared to static polymer foam stability. In this concern it would also be interesting to investigate any effect of polymer both in the bulk solution and in the interfaces.

Nomenclature

A	area (Darcy's law, equation 3.5)
A_G	area (surface tension definition, equation 2.1)
AOS	alpha olefin sulfonate
a_H	the horizontal area between the wells
B	bridging coefficient
BPR	back pressure regulator (Figure 15)
cmc	critical micelle concentration
DLVO	Derjaguin-Landau-Verwey-Overbekk theory
E	entering coefficient
epcap	exponent that control the capillary number's effect on the FM
epdry	regulates the slope of the relative permeability curve near the critical water saturation
epgcp	exponent that controls the capillary number's effect on the FM
epoil	exponent that controls the oil saturation's effect on the FM
epsurf	exponent that controls the surfactant concentration's effect on FM
F_1-F_6	dependent functions used in STARS
FAWAG	foam assisted water alternating gas
FM	dimensionless interpolation factor
FS-500	fluorinated surfactant
F_X	consists of 6 dependent functions F_1-F_6 that scale fmmob
f_{g*}	gas fractional flow at the transition between the two foam regimes
fmcap	the capillary number for reference foam
fmdry	the critical water saturation
fmgcp	the critical capillary number for foam generation
fmmob	reference mobility reduction factor used in STARS
fmoil	the maximum oil saturation for stable foam
fmsurf	the critical surfactant concentration
f_w	water fractional flow in the foam
g	gravity constant, 9,81 m/s^2
G	surface free energy
GOR	gas oil ratio
h	reservoir height (Figure 25)

I-A	Injection well in the North Sea field
k	permeability
k_{ri}	relative permeability of phase *i*
k_{rg}	relative permeability of gas
k_{rw}	relative permeability of water
k_z	permeability in vertical direction
L	lamella number
L_g	segregation length in a rectangular reservoir
M	mobility ratio
MRF	mobility reduction factor
N_c	capillary number
P	pressure (Figure 6)
P1	pressure tab 1, located at the inlet (Figure 15)
P2	pressure tab 2, located at the outlet (Figure 15)
P3	pressure tab 3, located 3/5 of the core length from the inlet (Figure 15)
P-1	production well 1 in the North Sea field
P-2	production well 2 in the North Sea field
dP	differential pressure (core flooding experiments)
p_A	pressure in phase A
p_B	pressure in phase B
p_c	capillary pressure
p_c^*	limiting capillary pressure
q_t	total injection rate
Q_i	injection rate of phase *i*
r	outer radius of the reservoir
R_1	principal radius 1
R_2	principal radius 2
r_g	segregation length in a cylindrical reservoir
S	spreading coefficient
SAG	surfactant alternating gas
S_o	oil saturation in the grid block
S_{orw}	residual oil saturation after water flooding
S_w	water saturation (in equation 4.3 used as water saturation in the grid block)
thinfac	function constant used in equation 4.3

v_g	gas velocity
vgcoef	gas velocity constant
vgexpn	gas velocity exponent
W_S	surfactant concentration in the grid block

Greek letters:

∇P	pressure gradient (Figure 20)
ΔL	length of porous media
Δp	pressure difference between phase A and phase B
ΔP	pressure drop (Figure 6)
ΔP_i	pressure across the porous medium for phase *i*
ΔP_{foam}	pressure across the porous medium with foam
$\Delta P_{no\text{-}foam}$	pressure across the porous medium without foam
$\Delta\rho$	density difference between water/surfactant solution and gas
λ_i	mobility of phase *i*
λ_1	mobility of fluid 1
λ_2	mobility of fluid 2
μ_g	gas viscosity
μ_i	viscosity of phase *i*
μ_w	water viscosity
Π	disjoining pressure isotherm
Π_E	electrostatic disjoining pressure isotherm (Figure 9)
Π_S	structural/steric forces disjoining pressure isotherm (Figure 9)
Π_T	total disjoining pressure isotherm (Figure 9)
Π_W	van der Waals forces disjoining pressure isotherm (Figure 9)
σ	surface/interfacial tension
σ_{AB}	surface/interfacial tension between phase A and phase B
$\sigma_{o/g}$	surface tension between oil and gas
$\sigma_{w/g}$	surface tension between water and gas
$\sigma_{w/o}$	interfacial tension between water and oil

References

Aarra, M. G. and Skauge, A., "A Foam Pilot in a North Sea Oil Reservoir: Preparation for a Production Well Treatment", SPE 28599, presented at the SPE 69th Annual Technical Conference in New Orleans, LA, 25-28 Sep., 1994.

Aarra, M. G., Skauge, A., Søgnesand, S., and Stenhaug, M., "A foam pilot test aimed at reducing gas inflow in a production well at the Oseberg Field", Pet. Geosci., 2 (1996) 125.

Aarra M. G., Ormehaug P. A., and Skauge A., "Foams for GOR Control: Improved Stability by Polymer Additives", presented at the 9th European Symposium on Improved Oil Recovery, The Hague, The Netherlands, 20-22 Oct., 1997, paper 10.

Aarra, M. G. and Skauge, A., "Status of foam applications in North Sea", 21st Annual International Energy Agency Workshop and Symposium, Edinburgh, Scotland, 19-22 Sep., 2000, paper 22.

Aarra, M. G., Skauge, A., and Martinsen, H. A., "FAWAG: A Breakthrough for EOR in the North Sea", SPE 77695, presented at the SPE Annual Technical Conference in San Antonio, TX, 29 Sep.-2 Oct., 2002.

Abed, M. A., Saxena, A., and Bohidar, H. B., "Micellization of alpha-olefin sulfonate in aqueous solutions studied by turbidity, dynamic light scattering and viscosity measurements", Colloids and Surfaces A, 233 (2004) 181.

Almgren, M. and Swarup, S., "Size of Sodium Dodecyl Sulfate Micelles in the Presence of Additives. 2. Aromatic and Saturated Hydrocarbons", J. Phys. Chem., 86 (1982) 4212.

Alvarez, J. M., Rivas, H. J., and Rossen, W. R., "Unified Model for Steady-State Foam Behavior at High and Low Foam Qualities", SPE 74141, SPE J., Sep. (2001) 325.

Arnaudov, L., Denkov, N. D., Surcheva, I., Durbut, P., Broze, G., and Mehreteab, A., "Effect of Oily Additives on Foamability and Foam Stability. 1. Role of Interfacial Properties", Langmuir, 17 (2000) 6999.

Atkins, P. W., Physical Chemistry, 6th ed., Oxford University press, New York, 1998.

Aveyard, R., Binks, B. P., Fletcher, P. D. I., Peck, T. G., and Garrett, P. R., "Entry and Spreading of Alkane Drops at the Air/Surfactant Solution Interface in Relation to Foam and Soap Film Stability", J. Chem. Soc. Faraday Trans., 89 (1993) 4313.

Bernard, G. G., Holm, L. W., and Jacobs, W. L., "Effect of Foam Trapped Gas Saturation and on Permeability of Porous Media to Water", SPE 1204, SPE J., Dec. (1965) 295.

Bikerman, J. J., Foams, Springer Verlag, New York, 1973.

Blaker, T., Aarra, M. G., Skauge, A., Rasmussen, L., Celius, H. K., Martinsen, H. A., and Vassenden, F., "Foam for Gas Mobility Control in the Snorre Field: The FAWAG Project", SPE 78824, SPEREE, Aug. (2002) 317.

Briggs, T., "Foams for Firefighting", in FOAMS: Theory, Measurements, and Applications, Prud'homme, R. K. and Kahn, S. A. (Eds.), Marcel Dekker, Inc., New York, 1996.

Brun, T. S., Høiland, H., and Vikingstad, E., "Partial Molal Volumes and Isentropic Partial Molal Compressibilities of Surfactant-Active Agents in Aqueous Solution", J. Colloid Interface Sci., 114, No. 1 (1978) 89.

Chen, M. and Yortsos, Y. C., "A Pore-Network Study of the Mechanisms of Foam Generation", SPE 90939, presented at the SPE Annual Technical Conference and Exhibition, Houston, TX, 26-29 Sep., 2004.

Cheng, L., Reme, A. B., Shan, D., Coombe, D. A., and Rossen, W. R., "Simulating Foam Processes at High and Low Foam Qualities", SPE 59287, presented at the SPE/DOE Improved Oil Recovery Symposium, Tulsa, OK, 3-5 Apr., 2000.

Christian, S. D. and Scamehorn, J. F., (Eds.), Solubilization in surfactant aggregates, Marcel Dekker, Inc., New York, 1995.

Chukwueke, V. O., Bouts, M. N., and van Dijkum, C. E., "Gas Shut-off Foam Treatments", SPE 39650, presented at the SPE/DOE Improved Oil Recovery Symposium, Tulsa, OK, 19-22 Apr., 1998.

Dalland, M., Hanssen, J. E., and Kristiansen, T. S., "Oil interactions with foams at static and flowing conditions in porous media", presented at the 13th IEA Collaborative Project on EOR Symposium, Banff (Alberta), 27-30 Sep., 1992.

Denkov, N. D., "Mechanisms of Foam Destruction by Oil-Based Antifoams", Langmuir, 20 (2004) 9463.

Derjaguin, B. V., Churaev, N. V., and Muller, V. M., Surface Forces, Consultants Bureau, New York, 1987.

Ettinger, R. A. and Radke, C. J., "Influence of Texture on Steady Foam Flow in Berea Sandstone", SPE 19688, SPERE, Feb. (1992) 83.

Evans, D. F. and Wennerström, H., THE COLLOIDAL DOMAIN, Where Physics, Chemistry, Biology, and Technology Meet, 2nd ed., Wiley-VCH, New York, 1999.

Exerowa, D. and Kruglyakov, P. M., Foam and Foam Films, Elsevier, Amsterdam, 1998.

Falls, A. H., Gauglitz, P. A., Hirasaki, G. J., Miller, D. D., Patzek, T. W., and Ratulowski, J., "Development of a Mechanistic Foam Simulator: The Population Balance and Generation by Snap-Off", SPE 14961, SPERE, Aug. (1986) 884.

Garrett, P. R., "Preliminary Considerations Concerning the Stability of a Liquid Heterogeneity in a Plane-Parallel Liquid Film", J. Colloid Interface Sci., 76 (1980) 587.

Garrett, P. R. (Ed.), "The Mode of Action of Antifoams" in Defoaming –Theory and Industrial application, Marcel Dekker, Inc., New York, 1993.

Gauglitz, P. A., Friedmann, F., Kam, S. I., and Rossen, W. R., "Foam Generation in Porous Media", SPE 75177, presented at the SPE/DOE Improved Oil Recovery Symposium, Tulsa, OK, 13-17 Apr., 2002.

Hanssen, J. E., Holt, T., and Surguchev, L. M., "Foam Processes: An Assessment of Their Potential in North Sea Reservoirs Based on a Critical Evaluation of Current Field Experience", SPE 27768, presented at the SPE/DOE Improved Oil Recovery Symposium, Tulsa, OK, 17-20 Apr., 1994.

Hirasaki, G. J., Miller, C. A., Szafranski, R., Lawson, J. B., and Akiya, N., "Surfactant/Foam Process for Aquifer Remediation", SPE 37257, presented at the International Symposium on Oilfield Chemistry, Houston, TX, 18-21 Feb., 1997.

Hirasaki, G. J., Miller, C. A., Szafranski, R., Tanzil, D., Lawson, J. B., Meinardus, H., Jin, M., Londergan, J. T., Jackson, R. E., Pope, G. A., and Wade, W. H., "Field Demonstration of the Surfactant/Foam Process for Aquifer Remediation", SPE 39292, presented at the SPE Annual Technical Conference and Exhibition, San Antonio, TX, 5-8 Oct., 1997[B].

Holm, L. W., "The Mechanism of Gas and Liquid Flow Through Porous Media in the Presence of Foam", SPE 1848, SPE J., Dec. (1968) 359.

Holt, T. and Vassenden, F., "Physical Gas/Water Segregation Model" in RUTH 1992-1995 Program Summary, Norwegian Petroleum Directorate, Stavanger, Skjæveland, S. M., Skauge, A., Hindraker, L., and Sisk, C. D. (Ed.), p. 75, 1996.

Holt, T. and Vassenden, T., "Reduced Gas-Water Segregation by Use of Foam", 9th European Symposium on Improved Oil Recovery, The Hague, The Netherlands, 20-22 Oct., 1997, paper 30.

Høiland, H. and Blokhus, A. M., "Solubilization in Aqueous Surfactant Systems", in Handbook of Surface and Colloid Chemistry, 2[ed], Birdi, K. S. (Ed.), CRC Press, Boca Raton, 2003.

Israelachvili, J. N., Intermolecular & Surface Forces, 2[ed], Academic Press, San Diego, 1991.

Jenkins, M. K., "An Analytical Model for Water/Gas Miscible Displacements", SPE 12632, presented at the SPE/DOE Enhanced Oil Recovery Symposium, Tulsa, OK, 15-18 Apr., 1984.

Khatib, Z. I., Hirasaki, G. J., and Falls, A. H., "Effects of Capillary Pressure on Coalescence and Phase Mobilities in Foams Flowing Through Porous Media", SPE 15442, SPERE, Aug. (1988) 919.

Koczo, K., Lobo, L., and Wasan, D. T., "Effect of Oil on Foam Stability: Aqueous Foams Stabilized by Emulsions", J. Colloid Interface Sci., 150 (1992) 492.

Kodama, M., "The Effect of the Alkali Metal Counter-ions on the Second CMC of Dodecyl Sulfates", J. Sci. Hiroshima Univ., Ser. A, 37, No. 1, (1973) 53.

Kovscek, A. R. and Radke, C. J., "Fundamentals of Foam Transport in Porous Media", in Foams: Fundamentals and Application in the Petroleum Industry, Schramm, L. L. (Ed.), American Chemical Society, Washington, DC, 1994.

Kruglyakov, P. M. and Vilkova, N. G., "The relation between stability of asymmetric films of the liquid/liquid/gas type, spreading coefficient and surface pressure", Colloids and Surfaces A, 156 (1999) 475.

Kuhlman, M. I., "Visualizing the Effect of Light Oil on CO_2 Foams", SPE 17356, J. Pet. Tech., July (1990) 902.

Kuhlman, M. I., Falls, A. H., and Wellington, S. L., "Gas/Oil Lamallae and Surfactant Propagation in the Oil in Carbon Dioxide Foam", SPE 27788, presented at the SPE/DOE Improved Oil Recovery Symposium, Tulsa, OK, 17-20 Apr., 1994.

Lake L. W., Enhanced Oil Recovery, Prentice Hall, New Jersey, 1989.

Lindman, B. and Wennerström, H., "Micelles, Amphiphile Aggregation in Aqueous Solution", in Topics in Current Chemistry, Volume 87, Boschke, F. L. (Ed.), 1980.

Lobo, L. and Wasan, D. T., "Mechanisms of Aqueous Foam Stability in the Presence of Emulsified Non-Aqueous-Phase Liquids: Structure and Stability of the Pseudoemulsion Film", Langmuir, 9 (1993) 1668.

Malliaris, A., "Effect of n-Alkane Additives on the Micellization of Ionic Surfactants", J. Phys. Chem., 91 (1987) 6511.

Manlowe, D. J. and Radke C. J., "A Pore-Level Investigation of Foam/Oil Interactions in Porous Media", SPE18069, SPERE, Nov. (1990) 495.

Mannhardt, K., Novosad, J. J., and Schramm, L. L., "Foam/Oil Interactions at Reservoir Conditions", SPE 39681, presented at the SPE/DOE Improved Oil Recovery Symposium, Tulsa, OK, 19-22 Apr., 1998.

Mannhardt, K. and Svorstøl, I., "Effect of oil saturation on foam propagation in Snorre reservoir core", J. Pet. Sci. Eng., 23 (1999) 189.

Mannhardt, K., Novosad, J. J., and Schramm, L. L., "Comparative Evaluation of Foam Stability to Oil", SPE 60686, SPEREE, Feb. (2000) 23.

Mannhardt, K. and Svorstøl, I., "Surfactant concentration for foam formation and propagation in Snorre reservoir core", J. Pet. Sci. Eng., 30 (2001) 105.

Marle, C. M., Multiphase flow in porous media, Editions Technip, Paris, 1981.

McAuliffe, C. D., "Oil and Gas Migration –Chemical and Physical Constraints", AAPG Bulletin, 63, No. 5 (1979) 761.

Meling, T. and Hanssen, J. E., "Gas-blocking foams in porous media: effects of oil and surfactant hydrophobe carbon number", Progr. Colloid Polymer Sci., 82 (1990) 140.

Miller, C. A., "Solubilization in Surfactant Systems", in Handbook of Surface and Colloid Chemistry, 2ed, Birdi, K. S. (Ed.), CRC Press, Boca Raton, 2003.

Nikolov, A. D., Wasan, D. T., Huang, D. W., and Edwards, D. A., "The Effect of Oil on Foam Stability: Mechanisms and Implications for Oil Displacement by Foam in Porous Media", SPE 15443, presented at the SPE Annual Technical Conference, New Orleans, LA, 5-8 Oct., 1986.

Nikolov, A. D. and Wasan, D. T., "Ordered Micelle Structuring in Thin Films Formed from Anionic Surfactant Solutions, -I. Experimental", J. Colloid and Interface Sci., 133, No. 1 (1989) 1.

Nikolov, A. D., Kralchevsky, P. A., Ivanov, I. B., and Wasan, D. T., "Ordered Micelle Structuring in Thin Films Formed from Anionic Surfactant Solutions -II. Model Development", J. Colloid and Interface Sci., 133, No. 1 (1989) 13.

Nishioka, G. M., Ross, S., and Kornbrekke, R. E., "Fundamental Methods for Measuring Foam Stability" in Foams: Theory, Measurements, and Applications, Prud'homme, R. K. and Khan, S. A. (Eds.), Marcel Dekker, New York, 1996.

Osterloh, W. T. and Jante Jr., M. J., "Effects of Gas and Liquid Velocity on Steady-State Foam Flow at High Temperature", SPE 24179, presented at the SPE/DOE Enhanced Oil Recovery Symposium, Tulsa, OK, 22-24 Apr., 1992.

Persoff, P., Radke, C. J., Pruess, K., Benson, S. M., and Witherspoon, P. A., "A Laboratory Investigation of Foam Flow in Sandstone at Elevated Pressure", SPE 18781, SPERE, Aug. (1991) 365.

Porte, G., Poggi, Y., Appell, J., and Maret, G., "Large Micelles in Concentrated Solutions. The Second Critical Micellar Concentration", J. Phys. Chem., 88 (1984) 5713.

Prud'homme, R. K. and Kahn, S. A., FOAMS: Theory, Measurements, and Applications, Marcel Dekker, Inc., New York, 1996.

Ransohoff, T. C. and Radke, C. J., "Mechanisms of Foam Generation in Glass-Bead Packs", SPE 15441, SPERE, May (1988) 573.

Raterman, K. T., "An Investigation of Oil Destabilization of Nitrogen Foams in Porous Media", SPE19692, SPERE, Aug. (1989) 329.

Romero, C., Alvarez, J. M., and Müller, A. J., "Micromodel Studies of Polymer Enhanced Foam Flow Through Porous Media", SPE 75179, presented at the SPE/DOE Improved Oil Recovery Symposium, Tulsa, OK, 13-17 Apr., 2002.

Rossen, W. R. and Zhou, Z. H., "Modeling Foam Mobility in Porous Media", SPE 22627, SPE Adv. Tech. Series, 3, No.1 (1995) 146.

Rossen, W. R., "Foams in Enhanced Oil Recovery", in FOAMS: Theory, Measurements, and Applications, Prud'homme, R. K. and Kahn, S. A. (Eds.), Marcel Dekker, Inc., New York, 1996.

Rossen, W. R., Zellinger, S. C., Shi, J.-X., and Lim, M. T., "Simplified Mechanistic Simulation of Foam Processes in Porous Media", SPE 57678, SPE J., Sep. (1999) 279.

Rossen, W. R. and van Duijn, C. J., "Gravity segregation in steady-stare horizontal flow in homogeneous reservoirs", J. Pet. Sci Eng., 43 (2004) 99.

Rowlinson, J. S. and Widom, B., Molecular Theory of Capillarity, Clarendon Press, Oxford, 1984.

Schramm, L. L. and Novosad, J. J., "Micro-Visualization of Foam Interactions with a Crude Oil", Colloids and Surfaces, 46 (1990) 21.

Schramm, L. L. and Novosad, J. J., "The destabilization of foams in improved oil recovery by crude oils: Effect of the nature of the oil", J. Pet. Sci. Eng., 7 (1992) 77.

Schramm, L. L., Turta, T., and Novosad, J. J., "Microvisual and Coreflooding Studies of Foam Interactions With a Light Crude Oil", SPE 20197, SPERE, Aug. (1993) 201.

Schramm, L. L. (Ed.), "Foam Sensitivity to Crude Oil in Porous Media", in Foams: Fundamentals and Application in the Petroleum Industry, American Chemical Society, Washington, DC, 1994.

Schramm, L. L. and Wassmuth, F., "Foams: Basic Principles" in Foams: Fundamentals and Application in the Petroleum Industry, Schramm, L. L. (Ed.), American Chemical Society, Washington, DC, 1994.

Schramm, L. L. (Ed.), Foams: Fundamentals and Application in the Petroleum Industry, American Chemical Society, Washington, DC, 1994[B].

Schramm, L. L. (Ed.), "Emulsions, Foams, and Suspensions: Fundamentals and Applications", Wiley-VCH, Weinheim, 2005.

Shan, D. and Rossen, W. R., "Optimal Injection Strategies for Foam IOR", SPE 88811, SPE J., June (2004) 132.

Shi, J.-X. and Rossen, W. R., "Simulation of Gravity Override in Foam Processes in Porous Media", SPE 35166, SPEREE, Apr. (1998) 148.

Shi, J.-X. and Rossen, W. R., "Improved Surfactant-Alternating-Gas Foam Process to Control Gravity Override", SPE 39653, presented at the SPE/DOE Improved Oil Recovery Symposium, Tulsa, OK, 19-22 Apr., 1998[B].

Skauge, A., Standal, S., Bøe, S. O., Skauge, T., and Blokhus, A. M., SPE 56673, presented at the SPE Annual Technical Conference and Exhibition, Houston, TX, 3-6 Oct.,1999.

Skauge, A., Aarra, M. G., Surguchev, L. M., Martinsen, H. A., and Rasmussen, L., "Foam-Assisted WAG: Experience from the Snorre Field", SPE 75157, presented at the SPE/DOE Improved Oil Recovery Symposium, Tulsa, OK, 13-17 Apr., 2002.

Speight, J. G., The chemistry and technology of petroleum, 3rd ed., Marcel Dekker, New York, 1998.

STARS users' guide, Computer Modeling Group, Calgary, Canada, 2005.

Stone, H. L., "Vertical conformance in an alternating water-miscible gas flood", SPE 11130, presented at the SPE Annual Technical Conference and Exhibition, New Orleans, LA, 26-29 Sep., 1982.

Stone, H. L., "A Simultaneous Water and Gas Flood Design with Extraordinary Vertical Gas Sweep", SPE 91724, presented at the SPE International Petroleum Conference in Mexico, Puebla Pue., Mexico, 7-9 Nov., 2004.

Suffridge, F. E., Raterman, K. T., and Russell, G. C., "Foam Performance Under Reservoir Conditions", SPE 19691, presented at the SPE Annual Technical Conference and Exhibition, San Antonio, TX, 8-11 Oct., 1989.

Surguchev, L. M., Søgnsand, S., Skauge, A., and Aarra, M. G., "Modeling and history matching of foam field pilot, Oseberg field", 8th European Symposium on Improved Oil Recovery, Vienna, Austria, 15-17 May, 1995, p. 29.

Svorstøl, I., Vassenden, F., and Mannhardt, K., "Laboratory Studies of a Foam Pilot in the Snorre Field", SPE 35400, presented at the SPE/DOE Improved Oil Recovery Symposium, Tulsa, OK, 21-24 Apr., 1996.

Vassenden, F. and Holt, T., "Experimental Foundation of Relative Permeability Modeling of Foam", SPE 39660, presented at the SPE/DOE Improved Oil Recovery Symposium, Tulsa, OK, 19-22 Apr., 1998.

Vassenden, F., Holt, T., and Solheim, A., "Foam Propagation on Semi-Reservoir Scale", SPE 39682, presented at the SPE/DOE Improved Oil Recovery Symposium, Tulsa, OK, 19-22 Apr., 1998[B].

Verwey, E. J. W. and Overbeek, J. Th. G., Theory of the Stability of Lyophobic Colloids, Elsvier, Amsterdam, 1948.

de Vries, A. S. and Wit, K., "Rheology of Gas/Water Foam in the Quality Range Relevant to Steam Foam", SPE 18075, SPERE, May (1990) 185.

Wasan, D. T., Koczo K., and Nikolov A. D., “Mechanisms of Aqueous Foam Stability and Antifoaming Action with and without oil” in Foams: Fundamentals and Application in the Petroleum Industry, Schramm, L. L. (Ed.), American Chemical Society, Washington, DC, 1994.

Xu, Q. and Rossen, W. R., “Effective viscosity of foam in periodically constricted tubes”, Colloids and Surfaces A, 216 (2003) 175.